FINAL REPORT

Designing Next Generation Polymer-Based Surfactants for Fire Suppression

SERDP Project WP18-1559

APRIL 2021

Timothy Long
Clay Arrington
Virginia Polytechnic Institute and State University

Gerard Back
Brian Lattimer
Jensen Hughes

SERDP
DOD ▪ EPA ▪ DOE

REPORT DOCUMENTATION PAGE

Form Approved
OMB No. 0704-0188

1. REPORT DATE *(DD-MM-YYYY)*	2. REPORT TYPE	3. DATES COVERED *(From - To)*
09-04-2021	SERDP Final Report	1/3/2019 - 1/3/2021

4. TITLE AND SUBTITLE

Designing Next Generation Polymer-Based Surfactants for Fire Suppression

5a. CONTRACT NUMBER
19-P-0001

5b. GRANT NUMBER

5c. PROGRAM ELEMENT NUMBER

6. AUTHOR(S)
Timothy Long, Clay Arrington, Gerard Back, Brian Lattimer

5d. PROJECT NUMBER
WP18-1559

5e. TASK NUMBER

5f. WORK UNIT NUMBER

7. PERFORMING ORGANIZATION NAME(S) AND ADDRESS(ES)
Virginia Tech
1040 Drillfield Drive
Blacksburg, VA 24061

Jensen Hughes Baltimore, MD 21227

8. PERFORMING ORGANIZATION REPORT NUMBER
WP18-1559

9. SPONSORING/MONITORING AGENCY NAME(S) AND ADDRESS(ES)
Strategic Environmental Research and Development Program (SERDP)
4800 Mark Center Drive, Suite 17D03
Alexandria, VA 22350-3605

10. SPONSOR/MONITOR'S ACRONYM(S)
SERDP

11. SPONSOR/MONITOR'S REPORT NUMBER(S)
WP18-1559

12. DISTRIBUTION/AVAILABILITY STATEMENT
DISTRIBUTION STATEMENT A. Approved for public release: distribution unlimited.

13. SUPPLEMENTARY NOTES

14. ABSTRACT
Current aqueous film-forming foams (AFFFs) employed for liquid fuel fire suppression by the military utilize perfluorinated compounds (PFCs) as surfactants. PFCs exhibit toxicity, bioaccumulation, and persistence in the environment, resulting in fluoro-containing surfactants in regions not directly exposed to PFCs but rather through secondary exposure by chemical migration. While fluorinated compounds provide desirable thermo-oxidative stability and excellent fire retardancy, the environmental impact imposed by these chemicals spurs research that targets the complete removal of PFCs in conventional surfactant formulations. In view of this, the design and synthesis of a series of wholly aromatic polyimides aims to replace PFCs in liquid fuel fire suppression. verall, the investigated systems performed well as stand-ins to AFFF but will require further development and optimization to realize a commercially accessible product.

15. SUBJECT TERMS
AFFF, PFAS, polyimide, poly(amic acid), fire suppression, replacement, polymeric surfactant,
Photocrosslinks, MIL-Spec, next generation

16. SECURITY CLASSIFICATION OF:			17. LIMITATION OF ABSTRACT	18. NUMBER OF PAGES	19a. NAME OF RESPONSIBLE PERSON
a. REPORT	b. ABSTRACT	c. THIS PAGE			Timothy Long
UNCLASS	UNCLASS	UNCLASS	UNCLASS	40	19b. TELEPHONE NUMBER *(Include area code)* 540-231-2480

Abstract: Designing Next Generation Polymer-Based Surfactants for Fire Suppression

Benjamin J. Stovall*, Clay B. Arrington*, Joshua B. Dinaburg[1], Gerard G. Back[1], Brian Lattimer[1,] and Timothy E. Long*

**Department of Chemistry, Macromolecules Innovation Institute (MII)*
Virginia Tech, Blacksburg, VA 24061
[1]Jensen Hughes, Baltimore, MD 21227

Current aqueous film-forming foams (AFFFs) employed for liquid fuel fire suppression by the military utilize perfluorinated compounds (PFCs) as surfactants. PFCs exhibit toxicity, bioaccumulation, and persistence in the environment, resulting in fluoro-containing surfactants in regions not directly exposed to PFCs but rather through secondary exposure by chemical migration. While fluorinated compounds provide desirable thermo-oxidative stability and excellent fire retardancy, the environmental impact imposed by these chemicals spurs research that targets the complete removal of PFCs in conventional surfactant formulations. In view of this, the design and synthesis of a series of wholly aromatic polyimides aims to replace PFCs in liquid fuel fire suppression (**Scheme 1**). The synthesized polyimides comprise highly thermally stable moieties that provide excellent fire resistance, high char yields, and highly rigid polymer backbones, yielding infusible materials. Likewise, the incorporation of metal-substituted sulfonate pendent groups enables water solubility for the rigid-rod polymers. Tailoring of the polyimide backbone through copolymerization with sulfonated and non-sulfonated monomers permits a family of polyimides to exhibit a balance of water solubility and flame suppression. When combined with non-toxic surfactants and salts in water, these sulfonated polyimides (sPI) have a high propensity for stable foam formation. The MIL-F-24385F performance requirement evaluates foam quality/stability, drainage time, and burn-back resistance to access viability and provides a comparison to other systems. To remove small molecule additives, sPI foam systems with backbone-tethered ammonium and phosphonium ion surfactants are also investigated. Overall, the investigated systems performed well as stand-ins to AFFF but will require further development and optimization to realize a commercially accessible product.

Scheme 1. Synthetic route to wholly aromatic, water-soluble polyimide

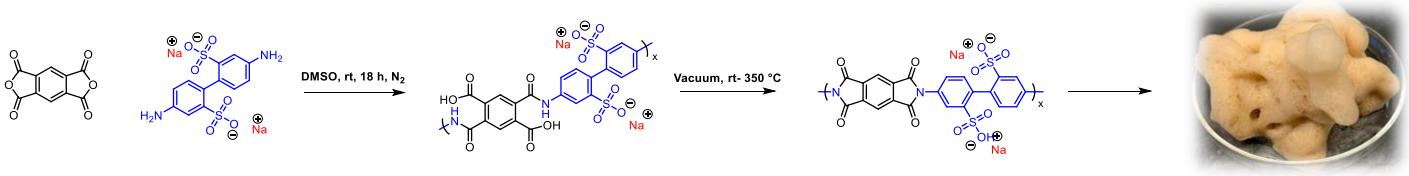

Table of Contents

List of Tables, Schemes, Figures

List of Acronyms, Initialisms

AFFF……..aqueous film-forming foam

PBT…… persistence, bioaccumulation, and toxicity

(s)PI…….(sulfonated) polyimide

(s)PAA……..(sulfonated) poly(amide acid)

BDSA……..4,4’-diamino diphenyl 2,2’-disulfonic acid

SDS……...sodium dodecyl sulfate

DMAEMA…….2-(dimethylamino)ethyl methacrylate

DMAE……...dimethylamino ethanol

TPO……diphenyl(2,4,6-trimethylbenzoyl)phosphine oxide

MTPP-Br……..methyltriphenylphosphonium bromide

DMSO……..dimethyl sulfoxide

DMF……...dimethylformamide

NMP…….…….. N-methyl-2-pyrrolidone

PMDA……....pyromellitic dianhydride

Keywords

AFFF, PFAS, polyimide, poly(amic acid), fire suppression, replacement, polymeric surfactant, Photocrosslinks, MIL-Spec, next generation

Acknowledgments

The authors would like to thank SERDP&ESTCP for their award and support throughout this research project, especially Dr. Robin Nissan and Braxton Lewis. The authors would also like to thank Lindsay Huffert at Jensen Hughes for her aid in testing the various foam formulations and Alan Kennedy with the US Army Engineer Research and Development Center (EDRC) for his expertise in testing and evaluating initial ecotoxicology.

Final Report: WP18-1559

Next Generation Poly(imide) and Poly(amic acid) Based Surfactants for Liquid Fuel Fire Suppression

Benjamin J. Stovall*, Clay B. Arrington*, Joshua B. Dinaburg[1], Gerard G. Back[1], Brian Y. Lattimer[1], and Timothy E. Long*

**Department of Chemistry, Macromolecules Innovation Institute (MII)*
Virginia Tech, Blacksburg, VA 24061
[1]Jensen Hughes
Baltimore, MD, 21227

Objective

A new fluorine-free foam platform will be developed through the proposed collaborative effort that is capable of meeting the fire suppression and environmental performance in MIL-F-24385F (NAVSEA, 1992). This work describes a new modular family of sulfonated polyimides containing flame-resistant aromatic sequences and imide linkages coupled with sulfonated units to impart water dispersibility/foaming and photo-crosslinkable sites to influence long-range flow. Testing is conducted to assess the foam fire suppression performance and environmental impact.

Introduction

The Aqueous Film Forming Foams (AFFFs) employed for Class B (liquid fuel) fire suppression by the military contain fluorinated surfactants, i.e., perfluorinated compounds (PFCs)) that impose several serious environmental impacts. The persistence, bioaccumulation, and toxicity (PBT) of these compounds resulted in the appearance of fluoro-containing surfactants in populations that were not directly exposed to AFFFs, but rather through chemical migration within the ecosystem.[1] Halogenated, specifically fluorinated surfactants provide desirable thermal stability and flammability resistance; however, their environmental impact suggests a necessary paradigm shift that completely removes halogenated sequences in conventional formulations. Currently, a limited number of fluorine-free foams exist on the market, but none meet the performance requirements for military applications (i.e., pass the fire performance set by MIL-F-24385F). Many efforts have been conducted to explore the replacement of fluoro-chemical surfactants with other organic and inorganic molecules. The early work in this area was performed with replacing the fluoro-chemical surfactant with xanthan gum, leading to the creation of the commercial fluorine-free foam RF6.[2,3] Though the exact formulation of RF6 is proprietary, it displays equivalent if not superior behavior to AFFF in several studies.[4,5] Examination of siloxane surfactants with and without a conventional surfactant enabled further development of fluorine-free AFFF replacements.[6] In small-scale fire testing, siloxane-based foams displayed enhanced performance compared to other commercially available fluorine-free foams but still fell short of sating MIL-F-24385F. Thus, the development of fluorine-free foams, which satisfy the fire suppression and environmental performance of MIL-F-24385F, remains a continued area of interest.

The excellent thermal stability, chemical resistance, insulating behavior, and thermomechanical performance of aromatic polyimides enables their wide application in the fields of aerospace and microelectronics. Conversely, perceived synthetic challenges limit the development of highly aromatic polyimides for aqueous applications. Continued development of

the disulfonic acid-containing polyimide monomers exhibited facile production of water-soluble polyamides.[7,8] In view of this, the design and facile synthesis of a family of aromatic polyimide and poly(amic acid) salts aimed to explore polymeric surfactants in liquid fuel fire suppression. The synthesized polymers comprise of highly thermally stable moieties which provide excellent fire resistance and highly rigid polymer backbones, yielding infusible materials.[9] Likewise, incorporation of sulfonate pendent groups based on 4,4'-diamino diphenyl 2,2'-disulfonic acid (BDSA) substituted with but not limited to monovalent metal cations, imparted water solubility for the rigid-rod polymers. Tailoring of the polymer backbone through copolymerization with sulfonated and non-sulfonated monomers permitted production of a modular family of poly(imide) and poly(amic acid)s exhibiting a balance of water solubility and synthetic ease. Formulation of the sulfonated poly(imide)s (sPIs) or sulfonated poly(amic acid) salts (sPAAs) with organic surfactants, glycolic ethers, and inorganic salts permits formation of stable aqueous foams. Analysis of the firefighting capacity and environmental impact of the sPI and sPAAs formulations has been undertaken to ascertain their performance as AFFFs.

Technical Approach

Materials: Sodium dodecyl sulfate (SDS) (Sigma Aldrich, 98%), sodium chloride (Fisher Chemical, certified ACS), 2-(dimethylamino)ethyl methacrylate (DMAEMA) (Sigma-Aldrich, 98%), diphenyl(2,4,6-trimethylbenzoyl)phosphine oxide (TPO) (97%, Sigma Aldrich), octylamine (Sigma Aldrich, 98%), hydrochloric acid (Fisher Chemical, certified ACS), deuterated chloroform (CIL, 99.8%), methyltriphenylphosphonium bromide (MTPP-Br) (98%, Acros Organics), Amberlite IRN-78 (Acros Organics) and deuterated dimethyl sulfoxide (DMSO- D6) (CIL, 99. %) were used as received. N, N-Dimethylacetamide anhydrous (Acros Organics, 99.5%), N, N-dimethylformamide (DMF) anhydrous (Acros Organics, 99.5%), dimethyl sulfoxide anhydrous (Acros Organics, 99.5%) and N-methyl-2-pyrrolidone anhydrous (NMP) (Acros Organics, 99.5%) were stored over activated molecular sieves. Pyromellitic dianhydride (PMDA) (Sigma Aldrich, > 98%), and 4, 4'-oxydianiline (ODA) (Acros, 98%) were sublimed before use. 2,2'-Benzidinedisulfonic acid (BDSA) (TCI, > 70 %) was dried and titrated with NaOH or LiOH and stored in a vacuum oven at 150 °C before use.

Analytical Methods: ^{1}H nuclear magnetic resonance (NMR) spectroscopy was performed at 25 °C using a Variant Unity 400 at 400 MHz. $CDCl_3$ or DMSO- D_6 served as the solvent for NMR analysis. Thermogravimetric analysis (TGA) was performed from 25 °C to 700 °C with a 10 °C/min heating rate and N_2 or air fill gas using a TA Instruments Q500. Differential scanning calorimetry (DSC) was conducted using a TA Instruments Q2000 DSC coupled with an RCS90 refrigerated cooling system and 50 mL/min N_2 cell purge. A heat/cool/heat procedure was utilized with 30 °C/min heating and cooling. Glass transition (T_g) values were determined from the second heat cycle via inflection point using TA Universal Analysis software. FTIR analysis was performed using a Nicolet iS5 equipped with an iD7 ATR (attenuated total reflection) stage at room temperature. Solution rheology was performed using a TA Instruments DHR-3 rheometer with a DIN cup and bob geometry in water at 23 °C. Photorheology was performed using a TA Instruments DHR-2 rheometer with 20 mm parallel plate geometry, UV curing accessory, and Omnicure S2000 light source equipped with a broad spectrum bulb and 320-500 nm filter. An oscillation procedure of 0.3 % strain and 4 Hz at 25 °C with a 500 µm gap was utilized during photorheology. Polymer solutions were subjected to oscillation for 30 s before UV irradiation with an intensity of 250 mW/cm^2 for 150 s.

Representative poly(amic acid) synthesis (50 mol% BDSA-Na). To a two-neck round bottom flask equipped with a magnetic stir bar and nitrogen inlet, BDSA-Na (0.1000 g, .0002575 mol) and ODA (0.0515g, 0.0002575 mol) were added. The flask was purged and backfilled with N_2 three times before addition of 15 mL of anhydrous DMSO. Following complete dissolution of the amines, PMDA (0.1123 g, 0.0005149 mol) was added to the solution with an additional 5 mL of DMSO. The resultant viscous solution was allowed to stir under nitrogen for 12 h before being stored in a refrigerator at 8 °C.

Film fabrication. Polyamic acid solution was allowed to warm to room temperature and was bladed on glass slide on a level surface without additional DMSO. The slide was then placed into a vacuum oven and kept at room temperature for 1 hour before being slowly ramped to 200 °C. The film was then held at 200 °C for 0.5 h and then transferred to a vacuum chamber residing in a metal bath. The chamber was then heated slowly to 350 °C and held at that temperature for 0.5 h. Films were then cooled slowly to room temperature and delaminated using acetone, and then dried at 60 °C overnight before analysis.

Representative sulfonated poly(amic acid) salt (sPAAS) formation: Addition of equal molar equivalents of DMAEMA to the carboxylic acid functionality of a poly(amic acid) polymerization solution permitted formation of carboxylate-ammonium interactions. Following 6 h of stirring at room temperature under air, the sPAAS solutions were diluted by half with DMSO before being precipitated into 50/50 (v:v) acetone/methanol. Post 4 h of stirring in the precipitation media, the solid powder was collected and subsequently washed with another 10x (by mass) of methanol. Filtering and drying under vacuum at room temperature enabled final isolation of the slightly yellow sPAAS powder.

Foam Formulation Testing and Characterization: New formulations were evaluated at the Jensen Hughes facility through a series of small-scale tests to quantify different suppression aspects of foam. This includes tests on expansion ratio and drainage, foam sealability, blanket degradation and ignition prevention under heat, foam flow over fuel, and burn-back resistance. The fuel used was gasoline. These formulations will be compared with the baseline performance of AFFF as well as commercially available RF6 foam solutions. For a complete description of tests and parameters, please refer to Appendix B.

Results and Discussion

1. Sulfonated Polyimides

Based on recent reports from the Long lab and other groups at Virginia Tech, telechelically functionalized polyimides did not display water solubility.[10–12] Therefore, investigation of pendant sulfonate groups aimed to facilitate water-soluble polyimides. As shown in **Scheme 1**, classical two-step polyimide formation enabled the production of a series of fully aromatic sulfonated polyimides.

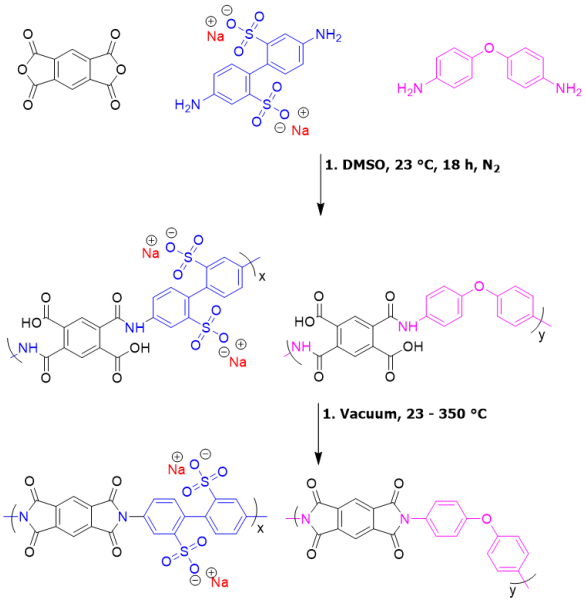

Scheme 1. Poly(amic acid) formation and thermal imidization of PMDA-ODA/BDSA-Na copolyimides. Variation of monomeric units enables the production of polymeric surfactants with an extensive range of functionality and properties.

Traditionally, polar aprotic solvents like NMP or DMAc accommodate PAA reactions[13]; however, to dissolve the BDSA-Na monomer, anhydrous DMSO was required. The PAA and thermal imidization procedure produced various copolyimide compositions from 0 -100 mol% of BDSA-Na with PMDA.

All of the sPI compositions produced free-standing films of various mechanical robustness. As the content of ODA increased, the cast polymer films became increasingly more robust and creasible. Copolyimides containing 100 mol% and 75 mol% BDSA gave very brittle, and increasable films; however, fully dried thin films of the sPIs exhibited flexibility and moderate creasibility. Loading the copolyimides at 3 wt.% in DI water ascertained the obtained water solubility (**Table 1**). Unsurprisingly, polymers with above 75 mol% BDSA-Na content exhibited excellent solubility in an aqueous solution at loadings comparable to and higher than current PFC loading in AFFFs in both PAA and PI forms. Over a few days, however, the 75 mol% polymers became less stable in solution, as evidenced by the crashing out of solids. 0 mol% and 25 mol% polymers were not water-soluble in either their PI or PAA (non-neutralized) forms. While the PAA of the 50 mol% BDSA-Na polymer was water-soluble, the PI was less so; it only appeared to swell.

BDSA-Na mol%	Polyamic acid solubility	Polyimide solubility	Dry polyimide Creasability
0	-	-	++
25	-	-	++
50	+	-	+
75	++	+	-
100	++	++	-

Table 1. Water solubility and creasability of sPI series of PMDA-BDSA-Na/ PMDA-ODA

Thermal analysis of the 50, 75, and 100 mol% BDSA-Na polymers elucidated the weight loss profile and attempted to probe glass transition temperatures. DSC yielded no observable transitions up to 400 °C for the sPIs. This result aligns with the glass transition of 0 mol% BDSA-Na being around 430 °C, as incorporation of the more rigid BDSA-Na monomer should increase glass transition temperatures.[9] TGA analysis of the water-soluble sPIs revealed reduced $T_{d,5\%}$ relative to the PMDA-ODA PI. Desulfonation around 450 °C results in a reduction in weight loss temperatures for the sulfonated PIs.[14] Additionally, the sPIs demonstrated high char yields (> 65%), indicating efficient formation of carbonaceous material during degradation. This high charring may be advantageous during flame suppression as high charring may reduce production of toxic degradation products. Likewise, the degradation products of polyimides are well characterized and known to mostly be comprised of gaseous materials.[15]

To probe the solution behavior of the 100 mol% sPI at various concentrations, solution rheology was conducted in a flow sweep using a concentric cylinder geometry. Concentrations of 1 to 15%(w/v) were tested to obtain zero shear viscosity (η_o) which is thusly converted to specific viscosity (η_{sp}) and plotted against concentration to give the plot in **Figure 2**. Though experiments are to be conducted, the fit is consistent with Rouse and Rubenstein's model predictions for polyelectrolyte solutions. At ~8%(w/v), the scaling relationship changes from $\eta_{sp} \sim C^{1.2}$ to $\eta_{sp} \sim C^{4.0,}$ indicating a transition from the semi-dilute entangled to entangled regimes. However, these scaling relationships suggest the presence of salts in the polymer solution without additional added salt. For reference, commercial AFFFs and FFFs come in standard concentrations of 3% and 6%. Future experiments regarding solution rheology include studying the effects of salts, and surfactants like sodium dodecyl sulfate (SDS) mentioned below.

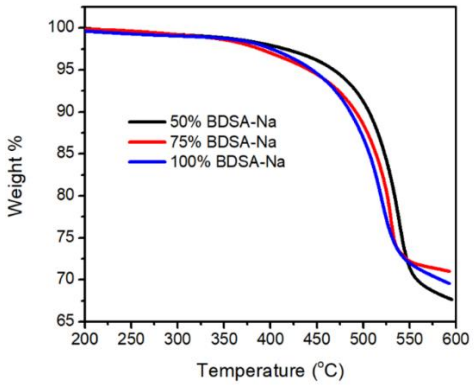

Figure 1. Thermogravimetric analysis of water-dispersible sPIs.

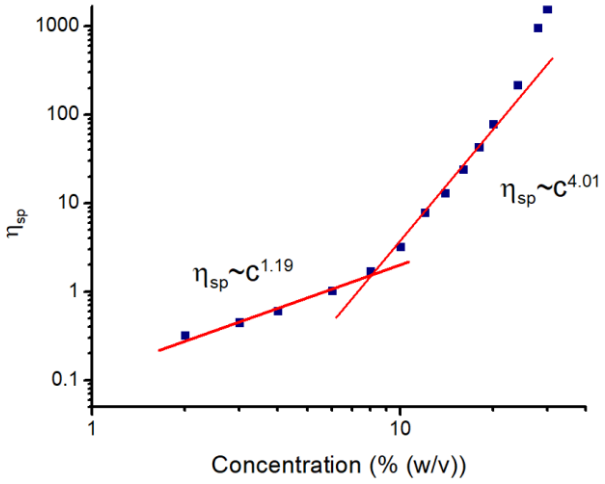

Figure 2. Solution Rheology of sPI (100 mol% BDSA-Na) plotted as specific viscosity, η_{sp}, vs. concentration.

Using the PMDA-BDSA-Na polymer, foam formulations were assessed. At 3 wt.% loading in water, minimal foaming was observed following agitation. However, the addition of 0.12 wt.% of a common commercial surfactant, sodium dodecyl sulfate (SDS), enabled the production of stable foams in the lab (Figure 2). The foams produced by SDS without PMDA-BDSA-Na displayed poor foamability and stability relative to the compounded formulation. Following production of the stable initial formulation, large-scale synthesis (~300 g of dried sPI) was done to produce a usable amount of polymer for industrial foam testing.

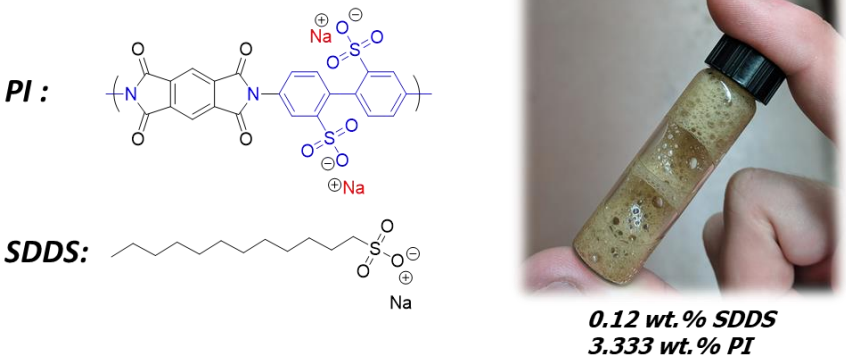

Figure 3. Aqueous sPI formulation components and foam produced by slight agitation

Additionally, initial testing of the sPI formulation shown in **Figure 3** with industrial partners at Jensen Hughes indicated meeting of MIL-Spec requirements for 25% drainage and expansion ratio. Foams were evaluated using Jensen Hughes procedures detailed in Appendix B. The tested formulation exhibited drainage times of 3.80±0.08 min and an average expansion ratio of

6.93±0.16 (**Figure 4**). Additionally, increasing the loading from 3 wt.% sPI to 6 wt.% sPI yielded a drainage time of 4.24 ±0.03 min and expansion of 6.19±0.09.

Figure 4. Foam drainage and expansion ratio testing at Jensen Hughes. Performed with 3%(w/v sPI (PMDA-BDSA-NA), 0.15%(w/v) sodium dodecyl sulfate (SDS) surfactant in water.

During initial flame suppression and burn-back testing of the 3 wt.% (Generation 1) and 6 wt.% (Generation 1, Revision 1) formulations on a 6" square pan containing hexane fuel, both formulations extinguished all but one corner of the pan, establishing suppression. The corner then reignited the rest of the pan by 70 s for both loadings of the sPI. Foam stability tests were not conducted. Further investigations looking into additives for augmenting burn-back resistance are underway. For example, development of surfactant tethered sPIs initially looks promising for enhanced foam performance. (**Figure 5**). This system aims to remove further the need for small molecule organic surfactants, which display high diffusion relative to macromolecules, enabling possible chemical migration.

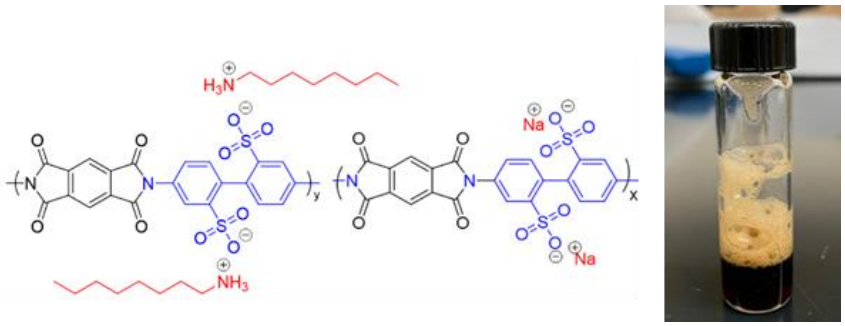

Figure 5. sPI copolymer with BDSA-OA/BDSA-Na has a higher propensity to foam compared to homopolymers of BDSA-Na and BDSA-OA without SDS surfactant.

Ecotoxicology of this "Generation 1" formulation was performed by the Army Engineer Research and Development Center (EDRC) in Vicksburg, MS. A 48 h Ceriodaphnia dubia acute

toxicity test was conducted for the 3% formulation, and the results can be seen in **Figure 6**. As it was preliminarily tested as a mixture, the cause for toxicity remains uncertain, but tests of the individual components are planned and being conducted. All concentrations are nominal, and the average LC50 expressed in terms of the polyimide is 216 mg/L. This places the toxicity in the practically non-toxic regime.

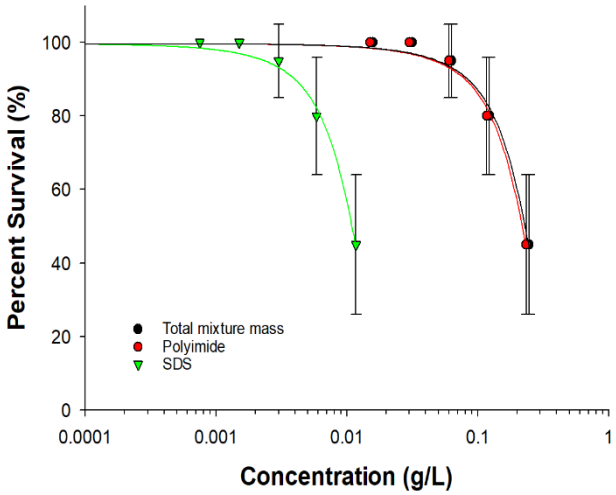

Figure 6. Ecotoxicology results of sPI foam formulation as reported by the Army EDRC

To enhance thermal stability, while focusing on previous flame retardancy methods, a BDSA monomer was developed with a tethered phosphonium moiety. Methyltriphenylphosphonium bromide (MTPP-Br) was used first due to its excellent water solubility and higher thermal stability (though thermal stability and flame retardancy can be mutually exclusive). MTPP-Br was converted to the OH form using Amberlite IRN-78, and MTPP-OH neutralized BDSA to give BDSA-MTPP in quantitative conversion (**Scheme 2**). Synthesis with this monomer did not result in water-soluble PAAs or PIs at 100 and 50 mol%. At 25 mol%, BDSA-MTPP produced a water-soluble polyimide, but the synthetic methodology is still being optimized. A large batch of the aforementioned formula (Generation 1) plus MTPP-Br was sent to Jensen Hughes to be tested as a control. The formulation (Generation 3) exhibited significant reductions in expansion and drainage time (not easily quantified on a small scale in the lab). The expansion ratio dropped from approximately 6 to approximately 5.5, and drainage fell below the MILSPEC requirement. This was also seen when MTPP-Br was added to Generation 4 material discussed below ("Generation 5"). The reduction of viscosity and foamability, as noticed by the engineers on a large scale, can be attributed to complex phenomena related to polyelectrolyte effects and polymer/surfactant/salt interactions in solution. While this is noticed for added MTPP-Br salts, phosphonium incorporation is not expected to have a similar effect when tethered to the polymer backbone.

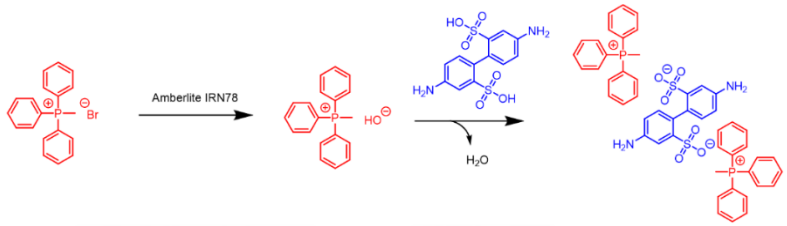

Scheme 2. Synthesis of BDSA-MTPP

2. Sulfonated Poly(amic acid) Salts

Investigation of sulfonated poly(amic acid) salts aimed to provide a less time-consuming, synthetic route for polymeric surfactant production, affording a second major pathway. The sPAAS utilize the same synthetic procedure as the sPI without requiring the second thermal imidization step. Following PAA formation, amine-containing DMAEMA facilitated neutralization to form the PAA salt (**Scheme 3**). Neutralization imparts two attributes to the PAA: increased hydrolytic and time stability via reduced intramolecular depolymerization[16] and improved water solubility via further inclusion of polar interaction along the backbone. Likewise, by tethering methacrylate functionality, the sPAAS are crosslinkable via radical polymerization.

The sPAAS display improved water solubility (50 mol% BDSA-Na readily dissolve at over 30 wt.% loading in water) relative to the imidized sPIs. Due to this, the 50 mol% BDSA-Na copoly(amic acid) was utilized for initial foam testing. Solutions of the sPAAS in water at 3 wt.% produced modest foaming; however, incorporating low wt.% (~ 0.3 wt.%) SDDS yielded stable foams that persisted in Petri dishes for ~ 25 min (**Figure 7**). Likewise, glycolic ethers and small molecular inorganic salts (i.e., NaCl) improved foam performance.

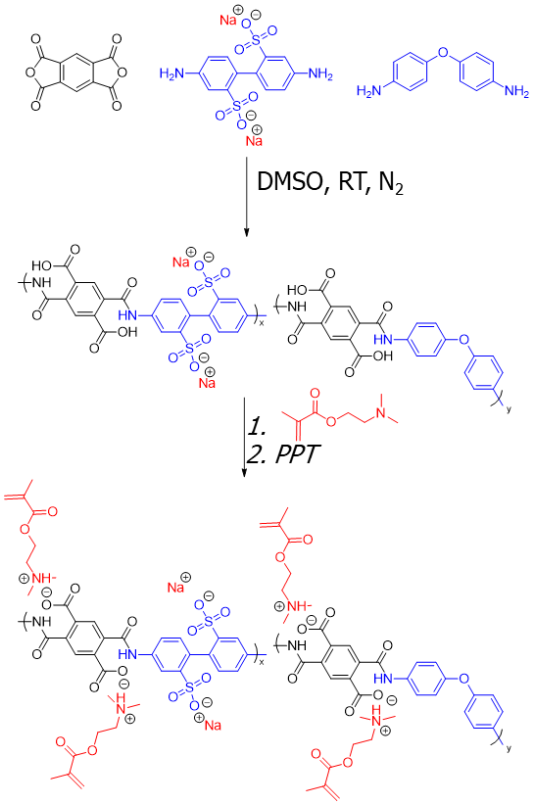

Scheme 3. Poly(amic acid) salt production using DMAEMA.

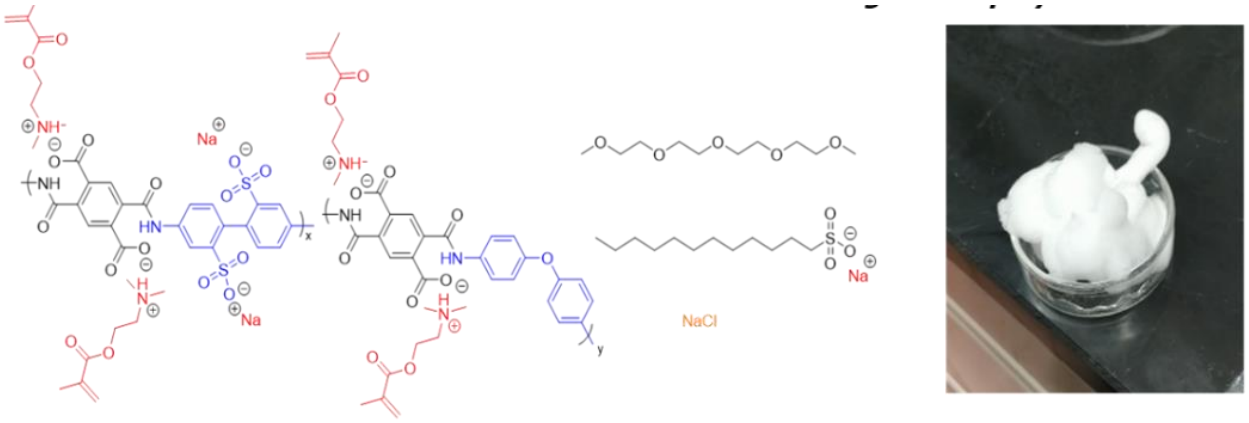

Figure 7. Aqueous sPAAS formulation components and foam. Amino acrylate units aim to provide crosslinking during flame suppression, combating migration of foams.

Inclusion of DMAEMA was hypothesized to improve charring through in-*situ* crosslinking during flame suppression. When coupled with a photoinitiator, sPAAS exhibit rapid photo-crosslinking and production of high strength hydrogels at 20 wt.% loading in water (**Figure 8**). From the photo-rheology, the sPAAS may be suitable for additive manufacturing using vat photopolymerization in water. Water-soluble, aromatic polyimide precursors for 3D printing would enable freeze-drying of printed hydrogels, permitting formation of aerogel materials for potential insulating applications.

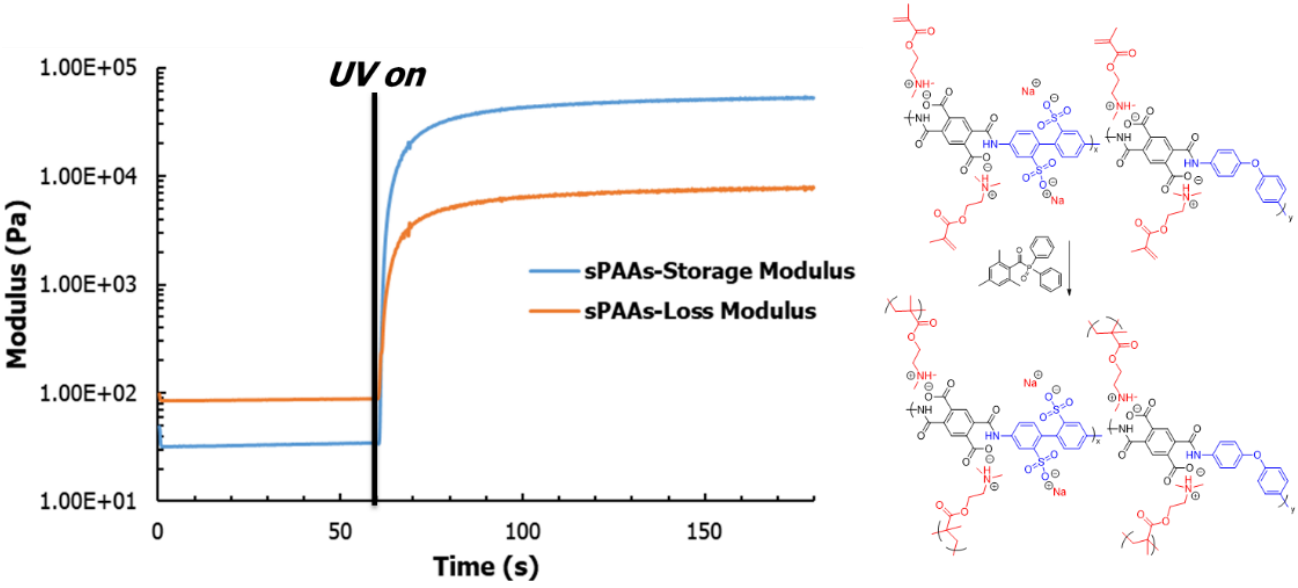

Figure 8. Photorheology of 20 wt.% sPAAS in water. Solutions produce rapid cross-over times and high moduli plateaus.

Poly(amic acid) salt-based formulation (3 wt.% PAAS, 0.3 wt.% SDS, Generation 2) produced similar expansion and drainage to previous formulations (6.5 and 7 min). For a 1 x 1 ft gasoline fire involving a 10 s pre-burn and application of 405 g of expanded foam (Test A,

Appendix B), the formulation could not extinguish the fire, hindering obtaining a burnback value, though it exhibited rapid fire control. Only small flamelets existed on the foam surface and edges after application. The ignition resistance of this formulation is greatly increased, however, attributed to chemical structure. Under higher radiant heating, 40 kW/m^2, thermal crosslinking of the polymer's acrylate sites delayed ignition by several minutes, with intermittent flashing and sustained flame (114 sec to flash, 134 sec to sustained ignition).

A similar poly(amic acid) salt, neutralized with dimethylaminoethanol (DMAE), was synthesized using the same synthetic methodology. The structure can be seen in **Figure 9.** The incorporation of DMAE instead of DMAEMA will ascertain the ability of the sPAAS system to be modified. The addition of DMAE will not only improve solubility but will allow for the controlling of the methacrylate concentration, which may affect fire control as C=C may react uncontrollably within a combustion environment producing many radical species.

As a control, a formulation of sPAAS neutralized with DMAE (0.15 wt% SDS in 3 wt% solution, Generation 4) gave an average expansion ratio of 7.14 and drainage time of 3.00 min, comparable to the previous test. 405 g of foam (approximately equal to 90 seconds of spray from the MILSPEC nozzle onto a 28 ft² MILSPEC fire, Test A, see Appendix B) almost extinguished a 1x1 ft gasoline fire apart from one corner and spread back to 25% in an additional 35 seconds. It prevented ignition on heated fuel for about 1 minute, and under 20kW/m^2, for about 2 minutes, both with flashing intermittently. This is quite promising as the performance was not hindered by the modifications and may help to act synergistically with Generation 2.

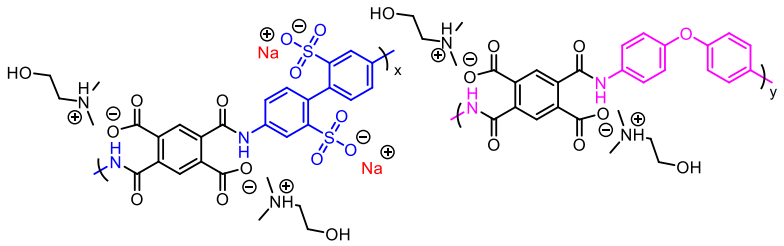

Figure 9. Structure of sPAAs neutralized with DMAE, Generation 4

Mixtures of various generations investigated any effects of mixing structure. First, Generation 1 and Generation 4 material (Generation 6) were mixed in an approximate 40:60 ratio(0.15wt% SDS, 3wt% solution), achieving an ER of 7.25 and drainage time of 3.02 min. Using Test A, burnback protocol (see Appendix B), this formulation (Generation 6) successfully extinguished a 1x1 gasoline pan fire in approximately 25 seconds, which none of the other generations achieved (**Figure 10)** Burnback, however, was deficient, as evidenced as after the addition of the burnback pan the fire spread to 25% coverage within 20 seconds. This is a similar performance as compared to other FFFs. In terms of foam stability on fuel surface, under 0 kW/m^2, the first ignition sustained at 1min 33 sec after adding the foam to the fuel, and under 20 kW/m2, it was 1 min 13 sec after heat added to flash ignition and 1 min 20 sec until sustained ignition.

Figure 10. Progression of extinguishment for Generation 6, from pre-burn to suppression/control to extinguishment

A mixture of Generation 2 and Generation 4 (0.3wt% SDS, 3wt% solution) attempted to elucidate effects of controlling acrylate concentration when exposed to a combustion environment (to reduce uncontrolled radical reactions in flame, allowing crosslinking due to heat boosting sealability, while other component helps in flame knockdown). The formulation, Generation 7, achieved an expansion ratio of 6.73 and a drainage time of 3.73 min, with extinguishment of a 1x1 gasoline pan fire (Test A, Appendix B). It exceeded the control of 30 seconds, however, extinguishing the fire in approximately 55 seconds and burn-back performance was more deficient; the pan was reignited almost immediately and reached 25% burn-back in approximately 15 seconds. Stability on fuel surface was approximately the same at 0 kW/m^2 compared to Generation 6 and about 25 seconds less for time to ignition under 20 kW/m^2.

Future Work

Assessment of the modified sPI and sPAAs at Jensen Hughes and additional large-scale synthesis, now that large-scale sPAAS and sPI techniques are in place, are paramount for determining optimal backbone structure for foam performance. With current synthetic techniques recently developed, rapid evaluation of aromatic polymeric surfactants is envisioned. Expansion of the currently employed monomeric units for sPI and sPAAS could lead to a host of polymeric surfactants with highly variable and advantageous properties as surfactants or waterborne coatings. Due to the highly charged nature of sPAAS, coupling of monomers which provide water solubility in the sPAAS state, but not when thermally converted to sPIs, may allow for coatings applied from water, which once cured, would display insolubility. Likewise, the inclusion of siloxane or other highly non-polar oligomeric diamines would allow for the synthesis of segmented sPIs and sPAAS, which may boast improved surfactant performance.

Future Pending Activities

- Further development and characterization of phosphonium neutralized sPIs
- Additional ecotoxicology of formulations and formulation components done at Army EDRC
- Continued collaboration with JH to evaluate foam properties and fire performance
- Development of sPI/PDMS segmented block copolymers to access the effects of PDMS incorporation on flame retardance and solution properties
- Optimization of successful formulations for further industrial evaluation

References:

(1) Reisch, M. S. The Price of Fire Safety. *C&EN Glob. Enterp.* **2019**, *97* (2), 16–19.
(2) Schaefer, T.; Dlugogorski, B.; Kennedy, E. Vapour Suppression of N-Heptane with Fire Fighting Foams Using Laboratory Flux Chamber. In *AOFST 7*; 2007; pp 1–12.
(3) Schaefer, T.; Dlugogorski, B.; Kennedy, E. Sealability Properties of Fluorine-Free Fire-Fighting Foams (FfreeF). *Fire Technol.* **2008**, *44*, 297–309.
(4) Hinnant, K. M.; Ursini, N.; Conroy, M.; Williams, B. A.; Ananth, R. Evaluating the Difference in Foam Degradation between Fluorinated and Fluorine-Free Foams for Improved Pool Fire Suppression. In *9th U.S. National Combustion Meeting, Central States Section of the Combustion Institute*; May 17-20, Cincinnati, OH, 2015; pp 1–10.
(5) Williams, B.; Murray, T.; Butterworth, C.; Burger, Z.; Fleming, J.; Whitehurst, C.; Farley, J. Extinguishment and Burnback Tests of Fluorinated and Fluorine-Free Firefighting Foams with and without Film Formation. In *Signaling Research and Applications - A Technical Working Conference (SUPDET 2011) 22-25 March 2011 Orlando, FL*; 2011; p 15.
(6) Hetzer, R. H.; Kümmerlen, F.; Wirz, K. A. I.; Blunk, D. Fire Testing a New Fluorine-Free AFFF Based on a Novel Class of Environmentally Sound High Performance Siloxane Surfactants. In *Fire Safety Science - Proceedings of the 11th International Symposium*; 2014; pp 1261–1270.
(7) Wang, Y.; Chen, Y.; Gao, J.; Yoon, H. G.; Jin, L.; Forsyth, M.; Dingemans, T. J.; Madsen, L. A. Highly Conductive and Thermally Stable Ion Gels with Tunable Anisotropy and Modulus. *Adv. Mater.* **2016**, *28* (13), 2571–2578.
(8) Wang, Y.; He, Y.; Yu, Z.; Gao, J.; ten Brinck, S.; Slebodnick, C.; Fahs, G. B.; Zanelotti, C. J.; Hegde, M.; Moore, R. B.; et al. Double Helical Conformation and Extreme Rigidity in a Rodlike Polyelectrolyte. *Nat. Commun.* **2019**, *10* (1).
(9) Sroog, C. E. Polyimides. *Prog. Polym. Sci.* **1991**, *16* (4), 561–694.
(10) Cao, K.; Stovall, B. J.; Arrington, C. B.; Xu, Z.; Long, T. E.; Odle, R. R.; Liu, G. Facile Preparation of Halogen-Free Poly(Ether Imide) Containing Phosphonium and Sulfonate Groups. *ACS Appl. Polym. Mater.* **2019**, acsapm.9b00938.
(11) Cao, K.; Serrano, J. M.; Liu, T.; Stovall, B. J.; Xu, Z.; Arrington, C. B.; Long, T. E.; Odle, R. R.; Liu, G. Impact of Metal Cations on the Thermal, Mechanical, and Rheological Properties of Telechelic Sulfonated Polyetherimides. *Polym. Chem.* **2019**.
(12) Cao, K.; Guo, Y.; Zhang, M.; Arrington, C. B.; Long, T. E.; Odle, R. R.; Liu, G. Mechanically Strong, Thermally Stable, and Flame Retardant Poly(Ether Imide) Terminated with Phosphonium Bromide. *Macromolecules* **2019**, *52* (19), 7361–7368.
(13) Ghosh, M. K.; Mittal, K. L. *Polyimides : Fundamentals and Applications*; Marcel Dekker, 1996.
(14) Liaqat, K.; Rehman, W.; Saeed, S.; Waseem, M.; Fazil, S.; Shakeel, M.; Kang, P. Synthesis and Characterization of Novel Sulfonated Polyimide with Varying Chemical Structure for Fuel Cell Applications. *Solid State Ionics* **2018**, *319*, 141–147.
(15) Hatori, H.; Yamada, Y.; Shiraishi, M.; Yoshihara, M.; Kimura, T. The Mechanism of Polyimide Pyrolysis in the Early Stage. *Carbon N. Y.* **1996**, *34* (2), 201–208.
(16) Herzberger, J.; Meenakshisundaram, V.; Williams, C. B.; Long, T. E. 3D Printing All-Aromatic Polyimides Using Stereolithographic 3D Printing of Polyamic Acid Salts. *ACS Macro Lett.* **2018**, *7* (4), 493–497.

Appendices

Appendix A: Scientific/ Technical Publications

- Stovall, B. J.; Arrington, C. B.; Dinaburg, J. B.; Back, G. G.; Lattimer, B. Y.; Long, T. E. *Designing Next Generation Polymer-Based Surfactants for Fire Suppression.* Presented at the 2019 SERDP and ESTCP Symposium, Washington, D.C., December 4, 2019. **Poster.**
- Stovall, B. J.; Arrington, C. B.; Dinaburg, J. B.; Back, G. G.; Lattimer, B. Y.; Long, T. E. *Designing Next Generation Polymer-Based Surfactants for Fire Suppression.* Presented at the 2019 Macromolecules Innovation Institute Technical Conference and Review, Virginia Tech, Blacksburg, VA, November 5, 2019. **Poster.**
- Long, T. E.; Hegde, M.; Arrington, C. B.; Stovall, B. J; Vandenbrande, J.; Wolfgang, J.; Dennis, J.; Meenakshisundaram, V.; Rao, D.; Williams, C.B. *Advances in High Temperature Polyimides: From 3D Printed Objects to Fire Suppression Foams*. Presented at the 40th High Temple Workshop, Sedona, AZ, February 6, 2020. **Presentation**
- Stovall, B. J.; Arrington, C. B.; Dinaburg, J. B.; Back, G. G.; Lattimer, B. Y.; Long, T. E. *Designing Next Generation Polymer-Based Surfactants for Fire Suppression.* Submitted online to the ACS Spring 2020 Virtual National Meeting and Exposition. April 2020. **Poster.**

Appendix B: Other Supporting Information

1. Guide of Polymer Generations and Revisions

Polymer Formulation	Description
Generation 1	**3 wt% sPI, 0.15 wt% SDS**
Generation 1, revision 1	**6 wt% sPI, 0.15 wt% SDS**
Generation 2	**3 wt% sPAAS with DMAEMA, 0.3 wt% SDS**
Generation 3	**3 wt% sPI, 0.15 wt% SDS, 0.3 wt% MTPP-Br, 0.3 wt%NaCl**
Generation 4	**3 wt% sPAAS with DMAE, 0.15 wt% SDS**
Generation 5	**3 wt% sPAAS with DMAE, 0.15 wt% SDS, 1 wt% MTPP-Br**
Generation 6	**3 wt% 40:60 sPI (Gen1): sPAAS with DMAE (Gen4), 0.15wt% SDS**
Generation 7	**3wt% 50:50 sPAAS with DMAEMA (Gen2): sPAAS with DMAE (Gen4), 0.3 wt% SDS**

2. Jensen Hughes Testing Protocol

Foam Quality

For this study, a critical characteristic was the quality of foam produced by the 2 GPM (7.6 LPM) MIL-SPEC nozzle. This nozzle is an aerated nozzle made from a modified National Foam Systems nozzle with a "wing-tip" spreader. Foam solution is pre-mixed and stored under pressure to produce a nozzle pressure of 100 pounds per square inch (psi) (689 kPA) (See MIL-PRF-24385F Section 4.7.5 "Foamability").

Measurement of foam expansion and drainage was conducted in accordance with the methods of NFPA 412, "*Standard for Evaluating Aircraft Rescue and Fire-Fighting Foam Equipment*," Test Method A with a foam sample collector with two measurement cylinders as shown in Figure 1 [1].

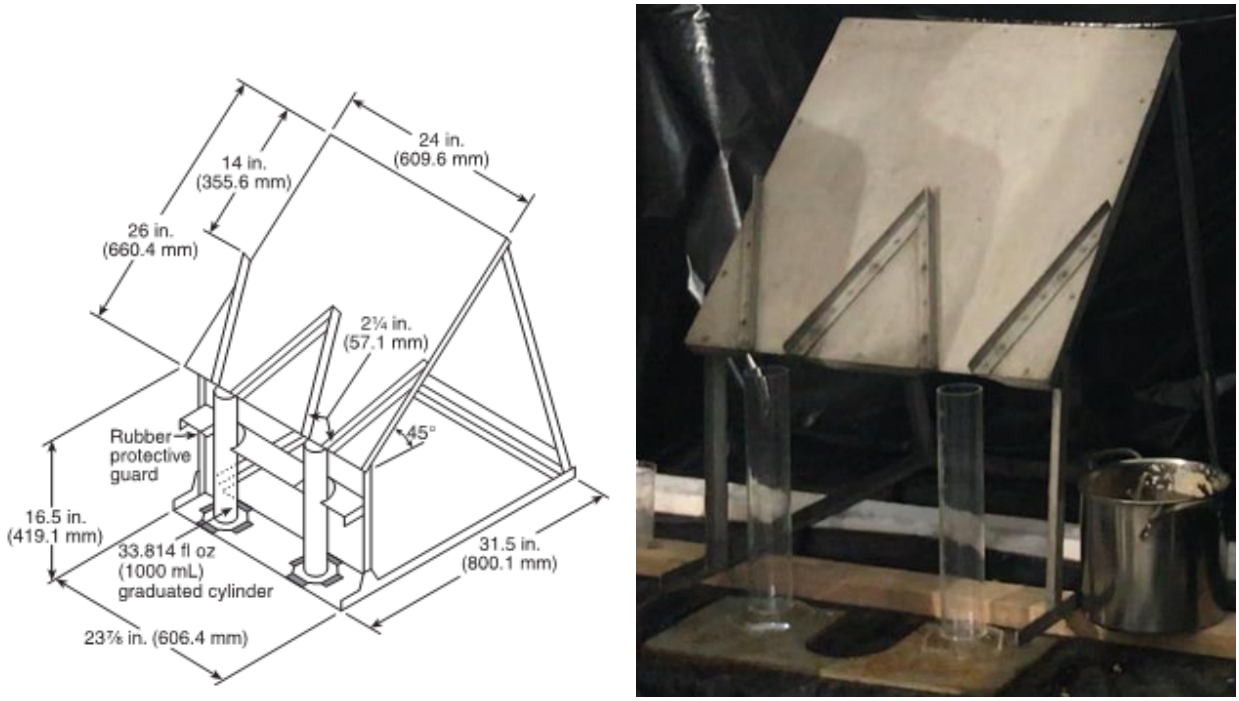

Figure 1– Foam sample collector schematic from NFPA 412 (left) [1] and photograph (right)

The foam is sprayed from the 2 GPM (7.6 LPM) nozzle from the hip at a distance of 4-6 ft (120-180 cm) onto the backboard. The foam then collects into the channels and fills the two 1000 mL graduated cylinders below. When full, the cylinders are removed, and the top surface scraped flat, and the outside wiped clean. The weight of the cylinder is measured to determine the expansion ratio of the foam, as the quotient of the volume (mL) and the mass (g). As liquid begins to drain from the foam, it collects at the bottom of the graduated cylinder. The 25% drainage time is determined by calculating 25% of the total foam mass and measuring the time until the liquid layer represents that amount of mass (1 g liquid = 1 mL).

MIL-SPEC has used the expansion ratio and drainage rates to characterize the quality of an AFFF foam. They require an expansion ratio greater than 5 and a 25 percent drainage time greater than 2.5 minutes. The quality of the foam is especially critical for the performance of FFFs that do not produce vapor retaining film. The real-world hardware and nozzles used to produce the foam can

greatly affect the performance of FFFs, although this topic is outside the scope of this study and has been explored elsewhere [2].

Matching Foam Quality for Small Scale Tests

A foam collector and separator were constructed to distribute foam into two flow paths, one containing 2/3 of the flow and the other with 1/3 of the flow. The fluidity testing was designed to utilize the 1/3 flow (0.66 GPM (2.5 LPM)) while the flow from the other channel could be collected and used for stability and extinguishing and burn-back testing simultaneously. The foam collector and separator are shown in Figure 2 and Figure 3. The angle of the diverter plate in the primary flow path in Figure 3 was adjusted to achieve the 2:1 flow split desired.

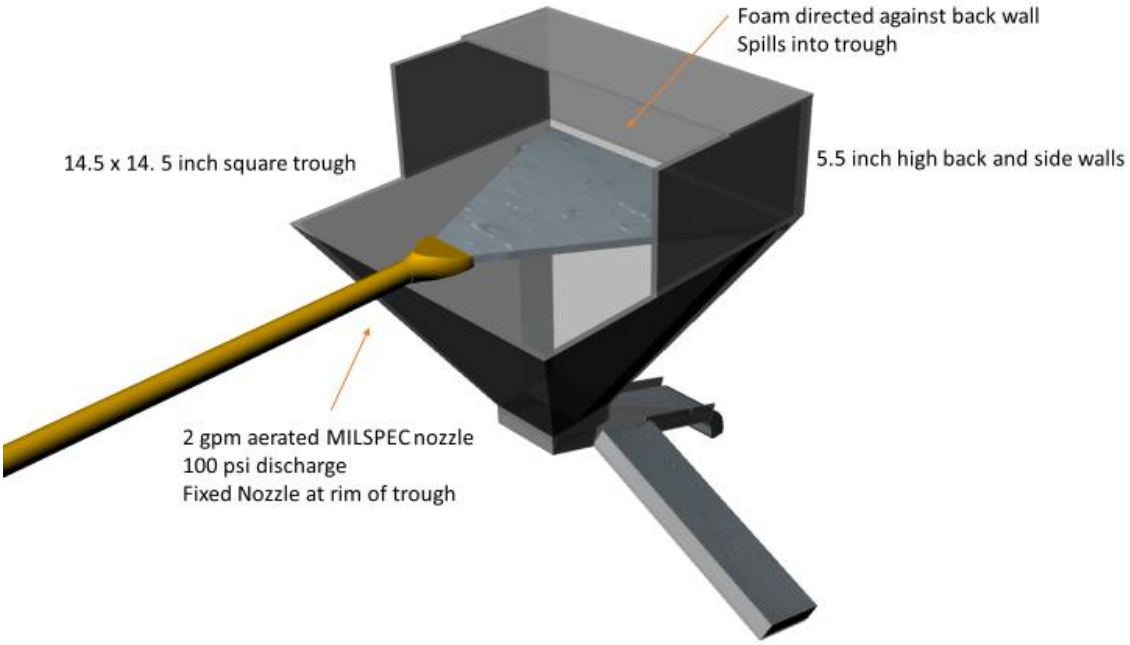

Figure 2 – Spray nozzle and foam collector and separator (front view)

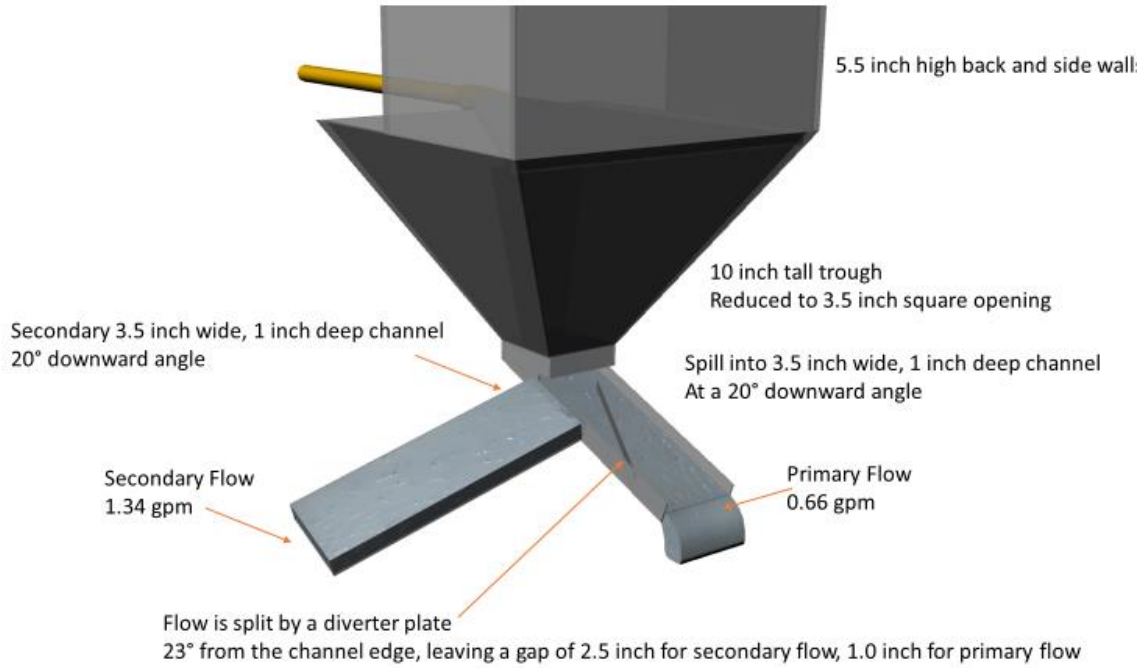

Figure 3- Spray nozzle and foam collector and separator (reverse view)

The foam collector and separator allowed for testing to be conducted using the 2 GPM (7.6 LPM) MIL-SPEC nozzle, ensuring equivalent foamability between the bench and MIL-SPEC testing while limiting the total consumption of foam. A full set of fluidity, stability, and extinguishing/burnback tests could be conducted with a total of approximately 1.5 gallons (5.7 L) of mixed foam solution (0.045 gallons (0.17 L) of 3% concentrate).

Fluidity

Fluidity Method

Fluidity tests were conducted by measuring the rate of area coverage of the foam provided from primary discharge of the foam collector and separator (see Section 3.1). Foam was discharged for a total of 20 seconds from the 2 GPM (7.6 LPM) nozzle and separated to provide 0.66 GPM (2.5 LPM) of foam to the fluidity test pan.

The fluidity test pan was a 24 x 45 in. (61 x 114 cm) steel pan 2 in. (5 cm) deep. The pan was separated with a vertical steel plate along the center line and provided with a semi-circular steel barrier at one end with a 12 in. (30.5 cm) radius. The splitter and circular barrier effectively doubled the length of the foam path and required the foam to change directions from its initial application directly, eliminating the impacts of discharge momentum for the second phase of spreading. The discharge and foam paths are shown in Figure 4 and Figure 5. The total wetted pan area was 7.07 ft² (0.66 m²), resulting in a total foam application density of 0.031 gal/ft² (1.27 L/m²). This is only slightly below the total application density required for extinguishing in the MIL-SPEC 28 ft² (2.6 m²) and 50 ft² (4.7 m²) pool fires, 0.036 gal/ft² and 0.033 gal/ft² (1.46 L/m² and 1.36 L/m²), respectively.

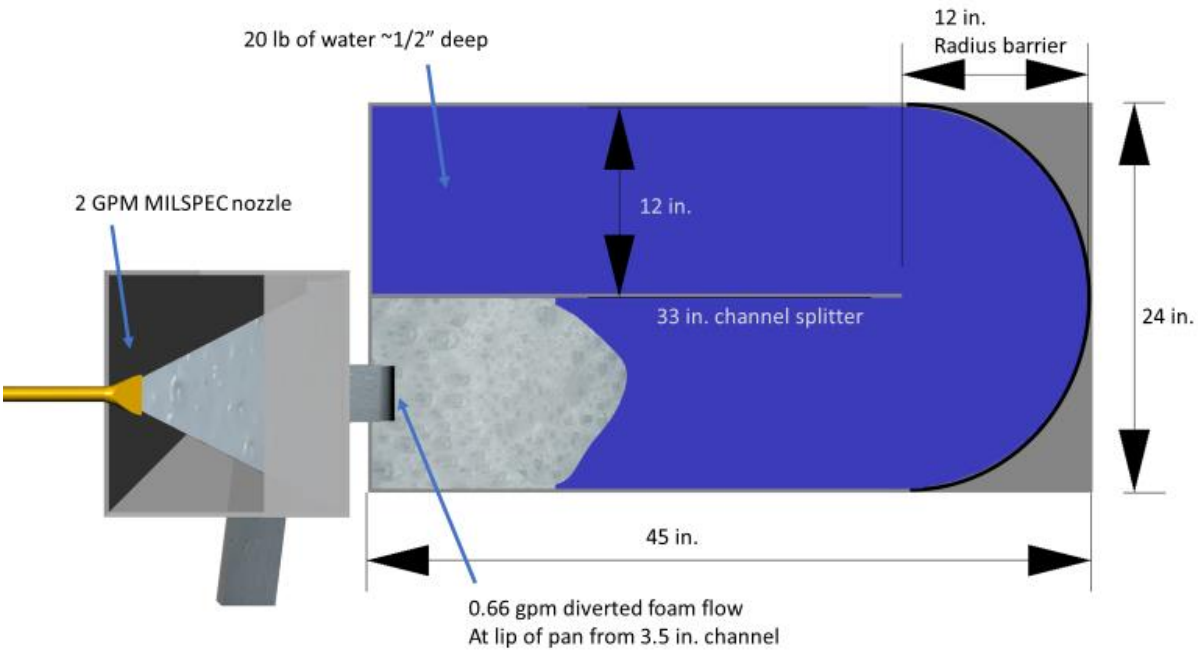

Figure 4– Foam fluidity test pan and foam distributor (top view)

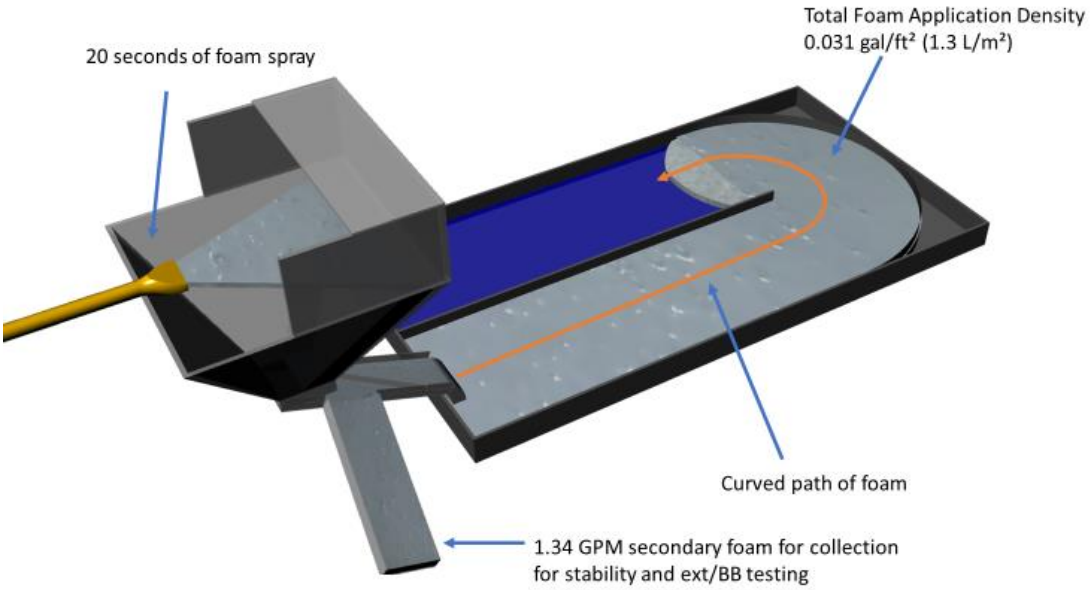

Figure 5– Foam fluidity test pan and foam distributor (foam spread view)

Fluidity Assessment

The pan is placed atop a Sartorius MISIUR-V1 load cell with 500 x 0.05 lbs (227 x 0.02 kg) capacity. The load cell is used to measure the mass of substrate water added to exactly 20.0 lbs (9.1 kg), resulting in a depth of approximately 0.5 in. (1.27 cm). This water depth has been shown in previous spread tests to be sufficiently deep to reduce the drag effects on the bottom of the pan [3]. In previous work on foam spread over liquid pools provided in the Appendix, water has been

shown to be a reasonable surrogate liquid surface to evaluate foam spread [3]. The load cell measured the rate and total amount of foam added to the test pan.

A Canon Vixia HF R800 video camera is mounted above the test pan, looking straight down. A customized video processing algorithm will be developed in Python to continuously measure the amount of surface area covered by the foam over the water. Each frame will be analyzed to get a continuous foam spreading rate, as shown in Figure 6. In addition to the coverage of thick, white foam, the area of the film/loose bubble layer in front of the foam blanket will also be measured.

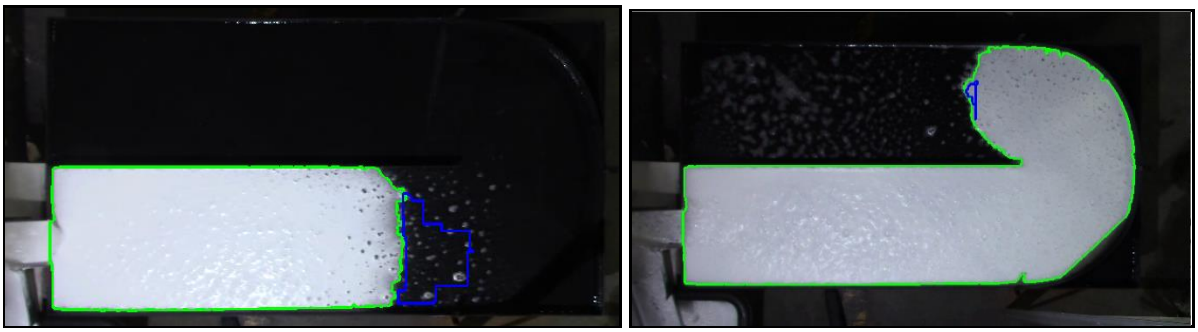

Figure 6– Video algorithm used to measure foam spreading area (green) and loose foam/film spreading (blue)

Prior to conducting fluidity testing, the camera will be calibrated to measure the area using a fixed grid of 0.79 x 0.79 in. (20 x 20 mm) black and white squares. This allowed for angular correction of area offset from the neutral camera axis. The calibration grid is shown in Figure 7. Foam spreading will be analyzed using the combined mass and area coverage rates to determine how quickly the area is covered as a function of both mass and time.

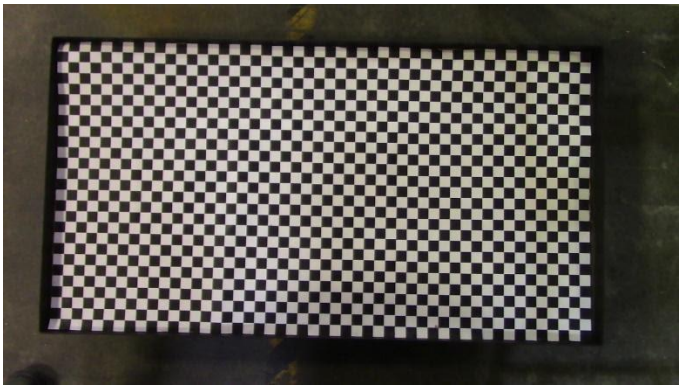

Figure 7– 20 x 20 mm grid used to calibrate video camera area analysis

Foam Stability

Vapor retention/stability tests were conducted by placing a layer of foam on top of gasoline and water. The gasoline used was ethanol-free gasoline in accordance with MIL-SPEC Section 4.7.10.1 conforming to ASTM D4814, "*Standard Specification for Automotive Spark-Engine Ignition Fuel*." [4]. A set of three quartz glass beakers with 0.165 ± 0.007 gal (625 ± 25 mL) capacity were used containing a layer of 2.36 in. (60 mm) of red-dyed water, a layer of 0.39 in. (10 mm) of gasoline, and a layer of 0.98 in. (25 mm) (initial thickness) of foam.

The foam applied was collected from the secondary flow channel of the collector and separator shown in Figure 3. The foam could be collected, and the stability tests conducted simultaneously with the fluidity test to reduce foam waste and limit the total amount of foam solution consumption. The foam was collected and then poured directly atop the test fuel to a depth of 0.98 in. (25 mm).

A small propane diffusion flame was positioned at the top edge of the beaker to ignite any fuel escaping fuel vapors, and the beaker was placed atop a Minebea Intec – Combics 2 load cell with 0.01 g resolution. The load cell continuously measured the amount of foam/vapor evaporated from the beaker.

Vapor Retention on Heated Fuel Method

The water in the beaker was preheated to a temperature of 50°C (122°F), and then the fuel and foam were added to the beaker, as shown in Figure 8. The fuel was not directly preheated to eliminate dangerous vaporization and unquantified mass loss. The thin layer of fuel was rapidly heated by the water below after application of the fuel and foam.

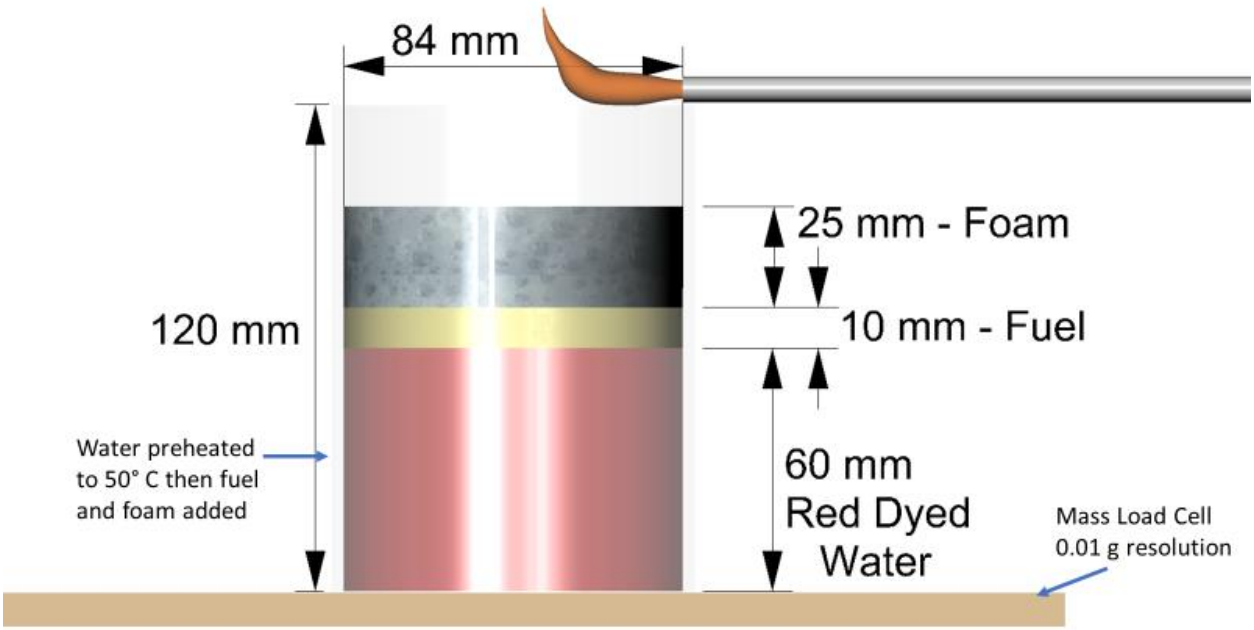

Figure 8– Test configuration for stability of foam on heated fuel

Stability of Foam Under External Radiation Method

These tests were conducted in a similar method as the heated fuel, but rather than preheating the water and fuel, all liquids were combined at ambient temperature. After placing the foam atop the fuel, the beaker was placed beneath a conical electric heater calibrated to provide fixed radiant heat flux at the top surface of the beaker.

The heater used was designed in accordance with ASTM E1354, "Standard Test Method for Heat and Visible Smoke Release Rates for Materials and Products Using an Oxygen Consumption Calorimeter" Section 6.2 [5]. The heater consisted of a 5000 W, 240 V electric heating rod wound into the shape of a truncated cone. The heater was encased on the outside with double-wall steel and packed with insulation fibers. This heater is designed to produce uniform (±2%) heat flux across a 2 x 2 in. (50 x 50 mm) area approximately 1 in. (25 mm) below the cone up to 100 kW/m². The cone temperature was controlled, and the heat flux at the top surface of the beaker was measured with a water-cooled and calibrated Schmidt-Boelter type total heat flux gauge. The flux at the top surface of the beaker was fixed at either 20 kW/m² or 40 kW/m² in separate tests. In the MIL-SPEC scale tests, it was expected that the foam performance would be more correlated with results at higher heat flux levels, which could exceed as much as 40 kW/m². This is consistent with the heat fluxes from flames back down onto the burning fuel surface [6], which is similar to the expected exposure of heat onto a foam blanket just established on a fuel surface. Testing was also conducted at a lower heat flux of 20 kW/m², which would be representative of heat flux from a fire burning adjacent to an established foam blanket, as is the case in the burnback test. The beakers containing water, fuel, and foam were placed beneath the heating cone, as shown in Figure 9.

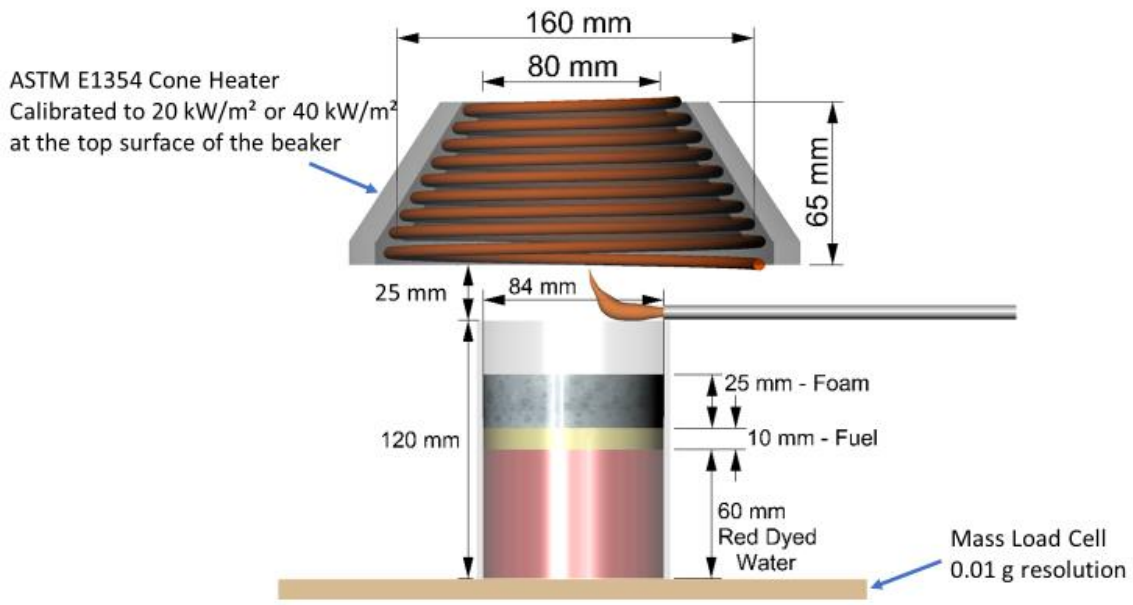

Figure 9– Test configuration for stability of foam exposed to external radiation from ASTM E1354 conical heater [5]

Stability Assessment

A Canon Vixia HF R800 video camera was mounted in a fixed position at the height of the water layer to view the water, fuel, and foam layers. A customized algorithm was developed in Python to analyze the test views to measure the height of the water (dyed red for visualization and contrast), the fuel, and the foam. Draining foam passes through the fuel layer and increases the volume of the dyed water layer. The depth of the water layer was used to determine the rate of mass drainage of the foam during exposure to the heated fuel. An example of the video analysis is shown in Figure 10. Note that the depth of the foam layer in the photograph increased from its

initial depth of 0.98 in. (25 mm) due to interaction with the heated fuel (swelling) and not due to additional foam application.

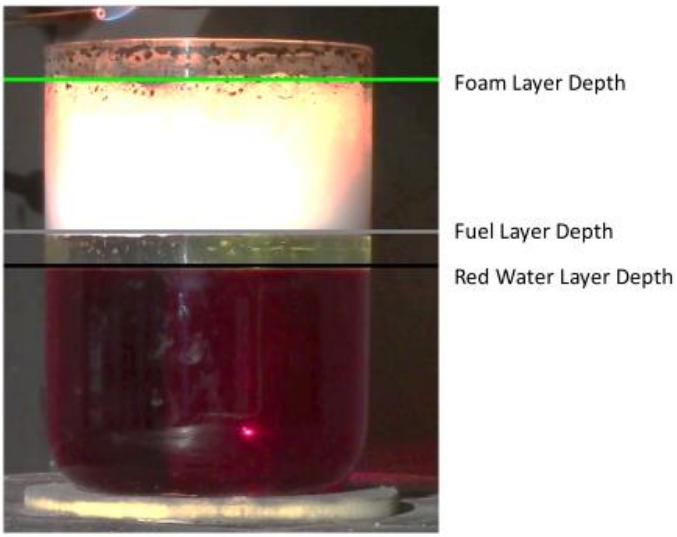

Figure 10– Foam stability video algorithm analysis of water, fuel, and foam depth

Foam thermal stability tests were evaluated using several metrics based on the times to achieve flashing and sustained ignitions, the total amounts of mass lost or drained at various time intervals, and the average rates of mass loss and drainage over time intervals. By analyzing the amount of mass evaporated and drained (and the sum of both) over the first 30, 60, and 180 seconds and over the entire test, a clearer picture was developed to indicate how the foam responded to the thermal stimuli over time. This broad array of metrics was evaluated to find the best indicators of MIL-SPEC scale fire performance using visual inspection and machine learning algorithm (MLA) analysis methods. The cumulative indicators (e.g., total amount of mass) are listed in Table 1. The average rates of mass loss/drainage were also calculated and are listed in Table 2.

Table 1– Cumulative metrics used to analyze thermal stability tests and correlate to MIL-SPEC performance

Time to flashing ignition (from SOT)	Mass of foam drained from 0 to 300 s (g)
Time to sustained ignition (from SOT)	Total mass of foam and fuel lost from 0 to 300 s (g)
Mass of foam and fuel evaporated from 0 to 30 s (g)	Mass of foam and fuel evaporated from 0 to onset of flashing ignition (g)
Mass of foam drained from 0 to 30 s (g)	Mass of foam drained from 0 to onset of flashing ignition (g)
Total (evaporation plus drainage) mass of foam and fuel lost from 0 to 30 s (g)	Total mass of foam and fuel lost from 0 to onset of flashing ignition (g)
Mass of foam and fuel evaporated from 0 to 60 s (g)	Mass of foam and fuel evaporated from 0 to onset of sustained ignition (g)
Mass of foam drained from 0 to 60 s (g)	Mass of foam drained from 0 to onset of sustained ignition (g)
Total mass of foam and fuel lost from 0 to 60 s (g)	Total mass of foam and fuel lost from 0 to onset of sustained ignition (g)
Mass of foam and fuel evaporated from 0 to 180 s (g)	Mass of foam and fuel evaporated in the 30 s before sustained ignition (g)

Mass of foam drained from 0 to 180 s (g)	Mass of foam drained in the 30 s before sustained ignition (g)
Total mass of foam and fuel lost from 0 to 180 s (g)	Total mass of foam and fuel lost in the 30 s before sustained ignition (g)
Mass of foam and fuel evaporated from 0 to 300 s (g)	(g) - grams

Table 2– Average rate metrics used to analyze thermal stability tests

Average rate of evaporation of foam and fuel from 0 to 30 s (g/s)	Average total rate of mass of foam and fuel lost from 0 to 300 s (g/s)
Average rate of drainage of foam from 0 to 30 s (g/s)	Average rate of evaporation of foam and fuel from 0 to onset of flashing ignition (g/s)
Average total rate of mass of foam and fuel lost from 0 to 30 s (g/s)	Average rate of drainage of foam from 0 to onset of flashing ignition (g/s)
Average rate of evaporation of foam and fuel from 0 to 60 s (g/s)	Average total rate of mass of foam and fuel lost from 0 to onset of flashing ignition (g/s)
Average rate of drainage of foam from 0 to 60 s (g/s)	Average rate of evaporation of foam and fuel from 0 to onset of sustained ignition (g/s)
Average total rate of mass of foam and fuel lost from 0 to 60 s (g/s)	Average rate of drainage of foam from 0 to onset of sustained ignition (g/s)
Average rate of evaporation of foam and fuel from 0 to 180 s (g/s)	Average total rate of mass of foam and fuel lost from 0 to onset of sustained ignition (g/s)
Average rate of drainage of foam from 0 to 180 s (g/s)	Average rate of evaporation of foam and fuel in the 30 s before sustained ignition (g)
Average total rate of mass of foam and fuel lost from 0 to 180 s (g/s)	Average rate of drainage of foam in the 30 s before sustained ignition (g)
Average rate of evaporation of foam and fuel from 0 to 300 s (g/s)	Average total rate of mass of foam and fuel lost in the 30 s before sustained ignition (g)
Average rate of drainage of foam from 0 to 300 s (g/s)	(g/s) – grams per second

Bench-Scale Extinguishing and Burnback

In addition to measuring the isolated processes that impact foam performance through fluidity and stability testing, a bench-scale test was developed to directly measure the combined ability of a foam to extinguish and prevent burn-back of a real flammable liquid fire. This test was designed to scale down and directly relate to the foam application used in the MIL-SPEC performance testing.

Extinguishing and Burnback Method

A set of increasingly challenging extinguishing and burn-back tests were conducted on a 1 x 1 ft (30.5 x 30.5 cm) square pan of water and fuel. The gasoline used was ethanol-free gasoline in accordance with MIL-SPEC Section 4.7.10.1 conforming to ASTM D4814 [4]. A total of 0.13 gal (500 mL) of fuel was placed atop a layer of 0.30 gal (1150 mL) of water (approx. 0.5 in. (12.7

mm) depth) of water in a steel pan 2 in. (50 mm) deep. The fuel was ignited and allowed to burn freely for either 10 or 20 seconds. Foam was then added to the fire at fixed masses to extinguish the fire. Additional foam was added after extinguishing before attempting to reignite the pool fire. The amounts of foam were designed to correlate with the amount of foam applied in the 28 ft² and 50 ft² (2.6 m² and 4.7 m²) extinguishing and burn-back tests in the MIL-SPEC.

The applied foam was collected from the secondary flow channel of the collector and separator shown in Figure 3. The foam could be collected, and the extinguishing test conducted simultaneously with the fluidity test and stability tests to reduce foam waste and limit the total amount of foam solution consumption. The foam was collected and weighed in a pourable pitcher to provide the exact mass specified.

The amount of foam applied was reduced in a series of increasingly more challenging extinguishing and burnback test scenarios. The first test, Test A, applied a mass of 405 g (0.89 lb) of foam directly to the fire after a preburn time of 10 seconds. Applying 405 g (0.89 lb) of foam to a 1 ft² (0.09 m²) pool fire results in the same application density as applying 90 seconds of foam from the 2 GPM (7.6 LPM) nozzle to the 28 ft² (2.6 m²) MIL-SPEC test fire (0.107 gal/ft² (4.36 L/m²)). The MIL-SPEC test fire is required to be extinguished during the first 30 seconds of discharge, and then burnback was conducted after applying an additional 60 seconds of foam discharge. The 405 g (0.89 lb) of foam represents the total amount of foam that would be applied during the combined 90 seconds.

The second most challenging test, Test B, utilized the same foam mass but splits the application into the first third, 136 g (0.30 lb), applied to achieve extinguishment of the pool fire (0.036 gal/ft² (1.46 L/m²)). The second 2/3 of the foam, 269 g (0.59 lb), was then applied after the fire was extinguished but before conducting a burn-back test. This test was specifically intended to replicate the amount of foam application density required for extinguishing and burnback in the MIL-SPEC pool fire.

Test C and Test D, the most challenging tests, reduced the foam application density to that required for extinguishment of the 50 ft² (4.7 m²) MIL-SPEC test fire. In that test, the fire must be extinguished before 50 seconds of application from the 2 GPM (7.6 LPM) nozzle, and burnback is tested after an additional 40 seconds of application. In both Tests C and D, 125 g (0.28 lb) of foam was applied to the 1 ft² (0.09 m²) pool fire to evaluate extinguishment (0.033 gal/ft² (1.35 L/m²)). After extinguishment, an additional 98 g (0.22 lb) of foam was added before attempting burnback. This is equivalent to the foam application density from the additional 40 seconds of discharge after extinguishment in the MIL-SPEC 50 ft² (4.7 m²) fire. Test D was made more challenging by allowing the pool fire to preburn for 20 seconds, compared to 10 seconds in Test C. The extra burn period resulted in higher initial fuel and pan temperatures, causing increased fuel vaporization.

The application of extinguishing and burnback foam applied for each of the four test conditions is summarized in Table 3. The depth of foam applied to the test fires for each scenario, based on estimated expansion ratios of 5.8 to 9.1, is shown in Table 4.

Table 3 – Extinguishing and Burnback Test Parameters

Test Class (Severity)	MIL-SPEC Pool Fire Test Basis	Pre-burn Time (s)	Foam Added for Ext. (g)	Foam Added After Ext. (g)	MIL-SPEC Test Basis
A (Least)	28 ft²	10	405	None	90 seconds of 2 GPM foam applied to 28 ft² pool fire
B	28 ft²	10	136	269	30 seconds of 2 GPM foam applied for extinguishment and 60 seconds applied for burnback of 28 ft² pool fire
C	50 ft²	10	125	98	50 seconds of 2 GPM foam applied for extinguishment and 40 seconds applied for burnback of 50 ft² pool fire
D (Most)	50 ft²	20	125	98	50 seconds of 2 GPM foam applied for extinguishment and 40 seconds applied for burnback of 50 ft² pool fire

Ext. - Extinguishing

Table 4 – Estimated depth of foam applied for extinguishing and burnback tests (expansion 5.8 – 9.1)

Method	Extinguishing Foam Depth (cm)	Total Burnback Foam Depth (cm)
Test A	2.5 – 4.0	2.5 – 4.0
Test B	0.8 – 1.3	2.5 – 4.0
Test C	0.8 – 1.2	1.4 – 2.2
Test D	0.8 – 1.2	1.4 – 2.2

During each test, the water and fuel were added to the pan at ambient conditions. Prior to ignition, adequate foam was collected from the secondary discharge, weighed, and stored in pourable vessels. The pool fire was then ignited and allowed to burn for the specified duration in Table 3. After the pre-burn, the extinguishing foam was rapidly poured from the vessel from an approximate height of 3 ft, or the intermittent peak height of the flames. The free burn and extinguishing foam applications are shown in Figure 11 and Figure 12, respectively.

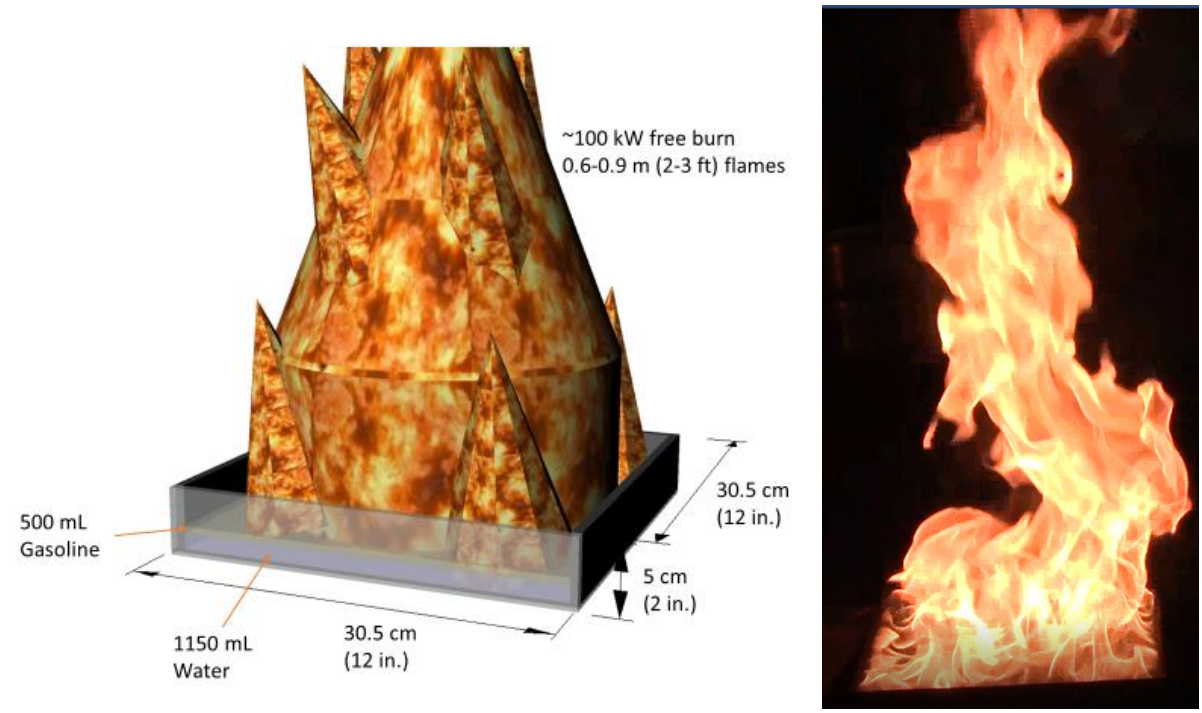

Figure 11 – Extinguishing Test – Free Burn

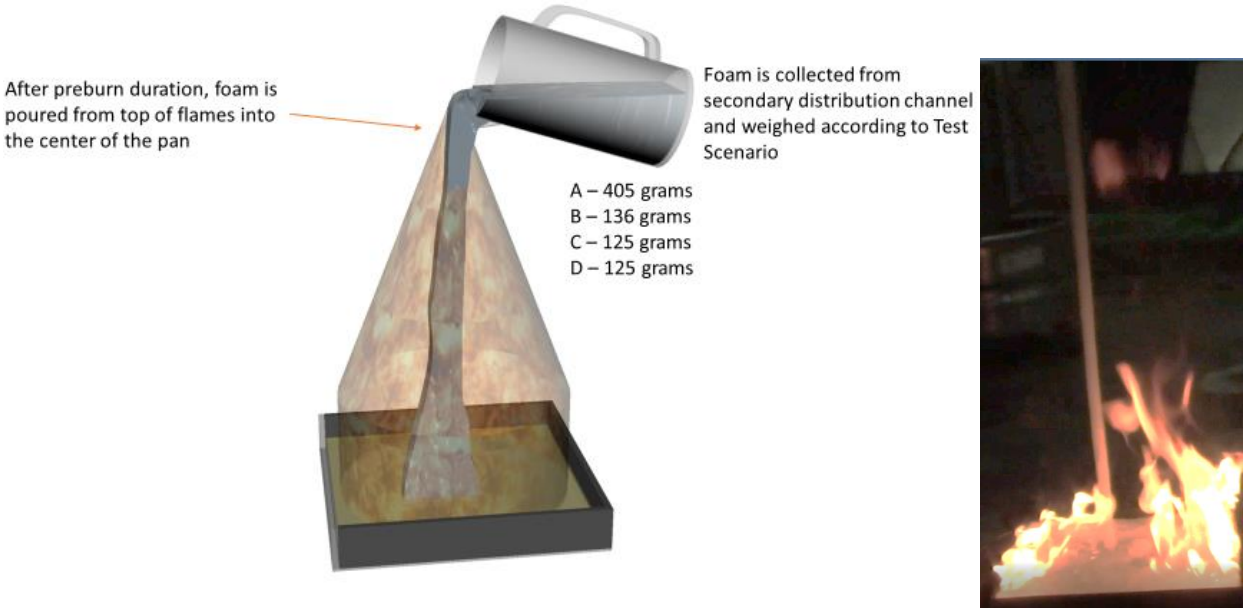

Figure 12 – Extinguishing Test – Foam Addition Stage 1

After applying the foam, the time was measured until all fire was extinguished. If all fire was not extinguished, the maximum extent of flame reduction was noted. Levels of reduction included; Control: (burning was noticeably reduced but was sustained in more than one corner), Suppression (burning was limited to a single flamelet in one corner), or No Control (no reduction in fire intensity) as shown in Figure 13.

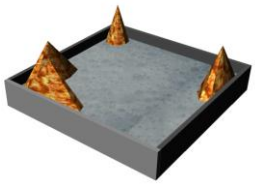	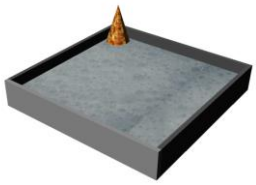	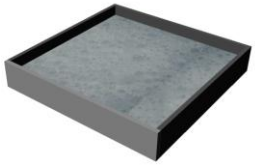
Control	**Suppression**	**Extinguished**

Figure 13 – Determination of control, suppression, and extinguishment

If the test scenario required a second addition of foam (Tests B, C, D), the remaining foam was added to the center of the pan immediately if the fire was uncontrolled or after 60 seconds from the maximum level of control/suppression/extinguishment.

The foam and hot fuel were left to drain/evaporate for 60 seconds after adding the second amount of foam. This is the maximum allowable time before initiating burn-back in MIL-SPEC testing. After 60 seconds, the burn-back pan was placed into the center of the test pan. The burnback pan was a round steel pan 8.5 cm (3.3 in.) in diameter and 3.9 cm (1.5 in.) deep, containing 15 mL of test gasoline. The burn-back pan was not allowed to sink below the level of the foam, or foam would spill in and extinguish the flames. For foams with a high expansion ratio, the depth of the foam layer could be taller than the burnback pan. In these cases, the burnback pan was held aloft using an attached wire and steel rod until the foam had receded to allow the pan to be placed down. Manual support of the burn-back pan is common practice in the MIL-SPEC scale testing as well. The initial burn-back test scenario is shown in Figure 14.

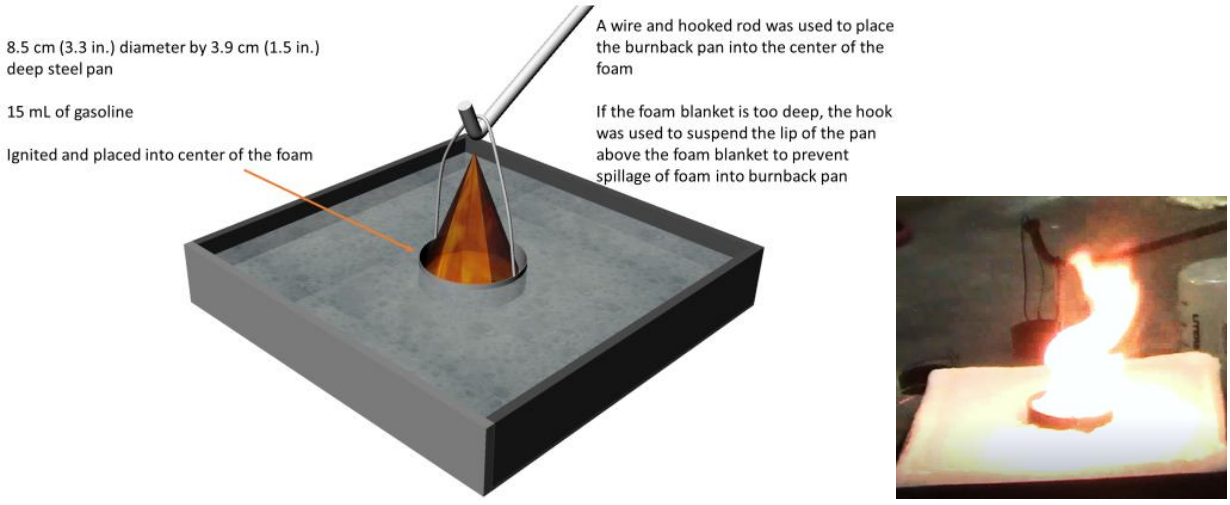

Figure 14 – Burnback Test – Insert Pan into foam

After a period of 5 minutes, the burnback pan was removed using the steel rod and wire. The operator would check if the pool was capable of sustained burning without the pan at this time. If sustained burning was observed, the burn-back pan was fully removed. If the residual pool was extinguished, the pan was returned to the test pan and checked again after 7.5 minutes. If sustained

burning still did not occur, the pan was returned and rechecked after 10 minutes. If the flames had visibly spread beyond the burnback pan prior to these removal times, it was removed. The removal of the burn-back pan is shown in Figure 15.

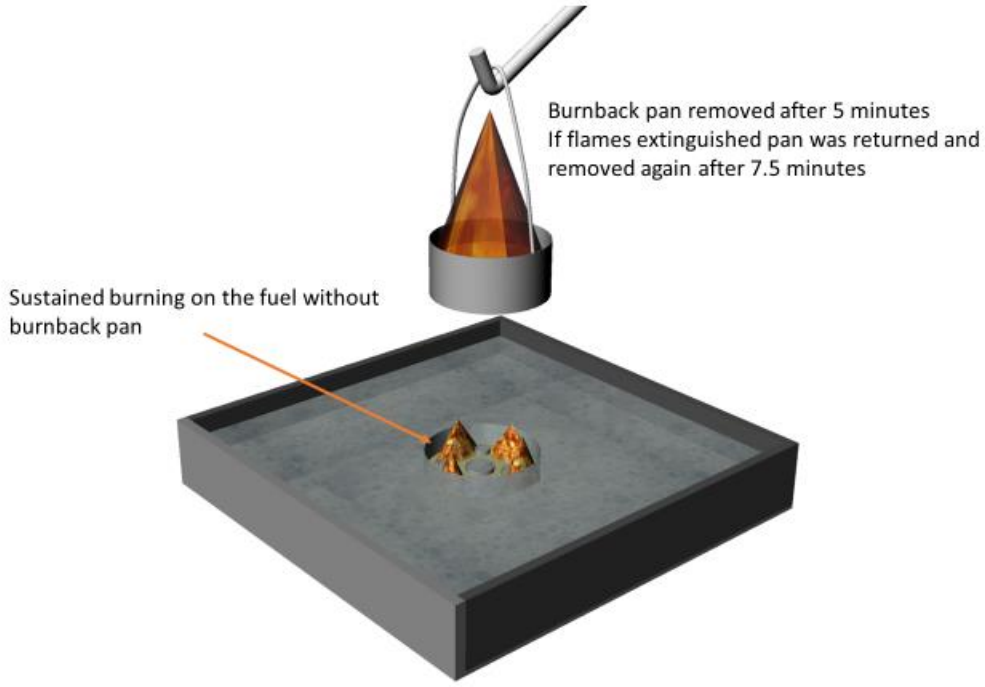

Figure 15 – Burnback test – Remove pan and check for sustained burning

The tests were continued until the original pool of fuel had reignited over 25% of the surface area. This is the same visual criteria used for burn-back evaluation in the MIL-SPEC standard. There was a noticeable increase in the radiant heat output of the flames at this time, and there was some qualitative certainty when 25% burn-back had occurred. The tests conducted at Jensen Hughes were observed by a technician with broad experience in judging 25% burn-back in full-scale tests. In addition, an open bead, Type K thermocouple, was placed above the pool at a height of 2 ft (61 cm). The thermocouple measured a sudden increase in temperature from below 100°C (212°F) to above 180°C (356°F) at the time of 25% burn-back. A more refined, quantitative metric may be developed for future test evaluation. Conceptual examples of 25% burn-back over the test pan area are shown in Figure 16, including an example with separate flaming areas contributing to the total 25%.

Figure 16 – Burnback test – examples of 25% pool area

The tests were continued until the original pool of fuel had reignited over 25% of the surface area or a maximum of 12 minutes. This is the same visual criteria used for burnback evaluation in the MIL-SPEC standard.

Extinguishing and Burnback Assessment

After applying the foam, the time was measured until all fire is extinguished. If all fire was not extinguished, the maximum extent of flame reduction would be noted. Levels of reduction include; Control: (burning is noticeably reduced but is sustained in more than one corner), Suppression (burning is limited to a single flamelet in one corner), or No Control (no reduction in fire intensity) as shown in Figure 17.

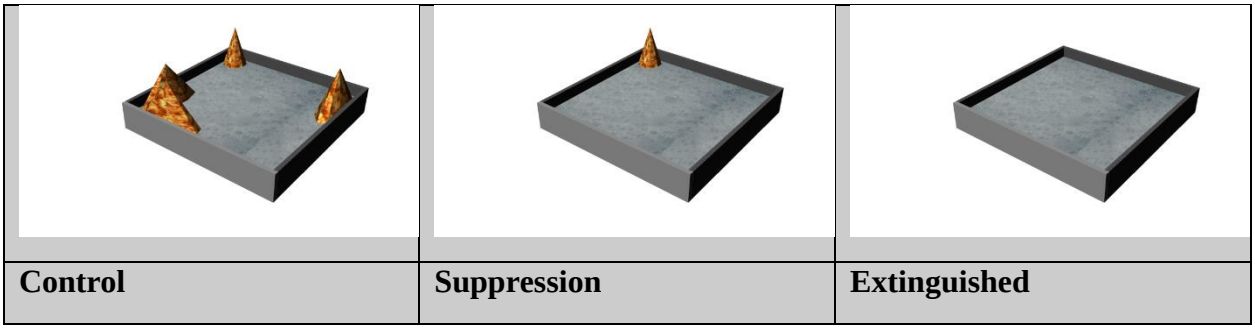

Figure 17– Determination of control, suppression, and extinguishment

A preliminary scoring system was developed for the analysis of the extinguishing test data. Scores were assigned of increasing value for achieving rapid extinguishment of the fire or by achieving control or suppression of fires from the first or second application of foams. The value of scores obtained from each successive test method was increased. The evaluation and scoring summary

for extinguishing tests is shown in Table 5. The scoring values from Table 5 were incrementally adjusted to provide the best correlation between bench-scale and MIL-SPEC extinguishing times.

Table 5 – Evaluation and scoring of extinguishing tests

TEST A	**Score**
NO CONTROL	0
CONTROL - FIRE IN MULTIPLE CORNERS OR AROUND EDGES	1
SUPPRESSION - FIRE NEARLY EXTINGUISHED BUT REMAINS IN 1 CORNER ONLY	5
EXTINGUISHED > 20 SECONDS	25
EXTINGUISHED <= 20 SECONDS	30
TEST B	**Score**
TEST NOT CONDUCTED - FAILED PREVIOUS TEST	0
APPLICATION 1 - NO CONTROL	0
APPLICATION 1 - CONTROL - FIRE IN MULTIPLE CORNERS OR AROUND EDGES	2
APPLICATION 1 - SUPPRESSION - FIRE NEARLY EXTINGUISHED BUT REMAINS IN 1 CORNER ONLY	10
APPLICATION 1 - EXTINGUISHED > 20 SECONDS	50
APPLICATION 1 - EXTINGUISHED <=20 SECONDS	60
APPLICATION 2 - NO CONTROL	0
APPLICATION 2 - CONTROL - FIRE IN MULTIPLE CORNERS OR AROUND EDGES	2
APPLICATION 2 - SUPPRESSION - FIRE NEARLY EXTINGUISHED BUT REMAINS IN 1 CORNER	10
APPLICATION 2 - EXTINGUISHED	50
TEST C	**Score**
TEST NOT CONDUCTED - FAILED PREVIOUS TEST	0
APPLICATION 1 - NO CONTROL	0
APPLICATION 1 - CONTROL - FIRE IN MULTIPLE CORNERS OR AROUND EDGES	2
APPLICATION 1 - SUPPRESSION - FIRE NEARLY EXTINGUISHED BUT REMAINS IN 1 CORNER ONLY	10
APPLICATION 1 - EXTINGUISHED > 30 SECONDS	50
APPLICATION 1 - EXTINGUISHED <=30 SECONDS	60
APPLICATION 2 - NO CONTROL	0
APPLICATION 2 - CONTROL - FIRE IN MULTIPLE CORNERS OR AROUND EDGES	2
APPLICATION 2 - SUPPRESSION - FIRE NEARLY EXTINGUISHED BUT REMAINS IN 1 CORNER ONLY	10
APPLICATION 2 – EXTINGUISHED	50

TEST D	Score
TEST NOT CONDUCTED - FAILED PREVIOUS TEST	0
APPLICATION 1 - NO CONTROL	0
APPLICATION 1 - CONTROL - FIRE IN MULTIPLE CORNERS OR AROUND EDGES	2
APPLICATION 1 - SUPPRESSION - FIRE NEARLY EXTINGUISHED BUT REMAINS IN 1 CORNER ONLY	10
APPLICATION 1 - EXTINGUISHED > 30 SECONDS	50
APPLICATION 1 - EXTINGUISHED <=30 SECONDS	60
APPLICATION 2 - NO CONTROL	0
APPLICATION 2 - CONTROL - FIRE IN MULTIPLE CORNERS OR AROUND EDGES	2
APPLICATION 2 - SUPPRESSION - FIRE NEARLY EXTINGUISHED BUT REMAINS IN 1 CORNER ONLY	10
APPLICATION 2 – EXTINGUISHED	50

The tests were continued until the original pool of fuel had reignited over 25% of the surface area. This is the same visual criteria used for burnback evaluation in the MIL-SPEC standard. There was a noticeable increase in the radiant heat output of the flames at this time, and there was some qualitative certainty when 25% burnback had occurred. The tests conducted at Jensen Hughes were observed by a technician with broad experience in judging 25% burnback in full-scale tests. In addition, an open bead, Type K thermocouple was placed above the pool at a height of 2 ft (61 cm). The thermocouple measured a sudden increase in temperature from below 100°C (212°F) to above 180°C (356°F) at the time of 25% burnback. A more refined, quantitative metric may be developed for future test evaluation. Examples of 25% burnback over the test pan area are shown in Figure 18, including an example with separate flaming areas contributing to the total 25%.

Figure 18– Burnback test – examples of 25% pool area

Works Cited

[1] NFPA 412, Standard for Evaluating Aircraft Rescue and Fire-Fighting Foam Equipment, Quincy, MA: NFPA, 2020.

[2] G. G. Back and J. P. Farley, "Evaluation of the fire protection effectiveness of fluorine free firefighting foams," Fire Protection Research Foundation, Quincy, MA, 2020.

[3] B. Lattimer and J. Scheffey, "Modeling of Aqueous Film Forming Foam (AFFF) Fire Extinguishment Performance," ONR Final Report, Contract No. N000014-02-C-00410, 2005.

[4] "ASTM D4814-20a Standard Specification for Automotive Spark-Ignition Engine Fuel," ASTM, West Conshohocken, PA, 2020.

[5] ASTM E1354-15a, "Standard Test Method for Heat and Visible Smoke Release Rates for Materials and Products Using an Oxygen Consumption Calorimeter," ASTM, West Conshohocken, PA, 2016.

[6] A. Tewarson, "Generation of Heat and Chemical Compounds in Fires," in *SFPE Handbook of Fire Protection Engineering*, 5th ed., 2016.